Theoretical Study of the Pyrolysis of Methyltrichlorosilane in the Gas Phase. 1. Thermodynamics

Yingbin Ge and Mark S. Gordon*

Department of Chemistry, Iowa State University, Ames, Iowa 50011

Francine Battaglia

Department of Mechanical Engineering, Iowa State University, Ames, Iowa 50011

Rodney O. Fox

Department of Chemical and Biological Engineering, Iowa State University, Ames, Iowa 50011

Received: August 23, 2006; In Final Form: November 27, 2006

Structures and energies of the gas-phase species produced during and after the various unimolecular decomposition reactions of methyltrichlorosilane (MTS) with the presence of H_2 carrier gas were determined using second-order perturbation theory (MP2). Single point energies were obtained using singles + doubles coupled cluster theory, augmented by perturbative triples, CCSD(T). Partition functions were obtained using the harmonic oscillator-rigid rotor approximation. A 114-reaction mechanism is proposed to account for the gas-phase chemistry of MTS decompositions. Reaction enthalpies, entropies, and Gibbs free energies for these reactions were obtained at 11 temperatures ranging from 0 to 2000 K including room temperature and typical chemical vapor deposition (CVD) temperatures. Calculated and experimental thermodynamic properties such as heat capacities and entropies of various species and reaction enthalpies are compared, and theory is found to provide good agreement with experiment.

I. Introduction

The chemical vapor deposition (CVD) of silicon carbide (SiC) has been widely studied experimentally and theoretically[1−38] due to its extraordinary physical and chemical properties. Two common crystal lattice structures of bulk SiC are α-SiC (wurtzite-type SiC) and β-SiC (zinc blende or diamond lattice SiC). Each Si (C) atom bonds with 4 C (Si) atoms tetrahedrally in both α-SiC and β-SiC crystals. Figure 1 shows that the major structural difference between the α and β forms of SiC is the six-member rings in α-SiC can adopt both boat and chair conformations, whereas only six-member rings with the chair conformation can be found in β-SiC, the major form of SiC produced by CVD. The high melting point (ca. 2700 °C),[39] satisfactory hardness (Moh's hardness of SiC is 9.3/10),[40] imperviousness to gaseous fission products, lower reactivity to oxygen compared with pure bulk Si, and relatively low cost of β-SiC make it an effective and economic coating material. One important use of SiC is as one of the TRISO (Tri-isotropic) coatings for the uranium kernels used as the nuclear energy fuel in high-temperature gas-cooled nuclear reactors. The TRISO coating consists of four layers: (1) the porous carbon buffer whose role is to accommodate fission products and fuel kernel swelling during and after the nuclear reactions; (2) pyrolytic carbon that traps fission products and prevents the first amorphous C layer from being chlorinated when undergoing the SiC coating process. (3) the β-SiC layer, which functions as a "pressure vessel" layer and is impervious to gas and metal fission products; (4) a pyrolytic carbon layer that provides protection for the SiC layer and the entire pellet.

* Corresponding author. Tel: 515-294-0452. Fax: 515-294-0105. E-mail: mark@si.fi.ameslab.gov.

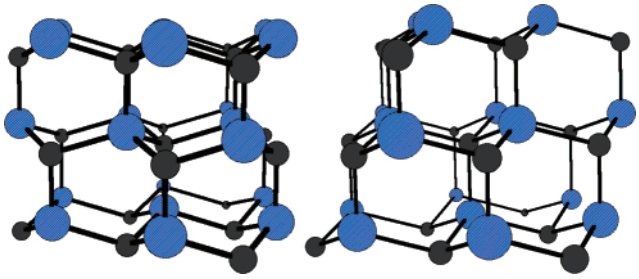

Figure 1. (Left) $Si_{20}C_{19}$ fragment of α-silicon carbide (wurtzite-type) structure, where the solid dark gray balls are C atoms and the balls with blue strips are Si atoms. (Right) $Si_{16}C_{19}$ fragment of β-silicon carbide (zinc blende or diamond lattice) structure. C and Si atoms on the surfaces have 1 or more dangling bonds.

The objective of this paper is to help clarify the mechanism of the SiC deposition.

Experiments have provided evidence that methyltrichlorosilane (MTS) is an ideal precursor for producing high quality β-SiC by using the CVD technique.[18] One possible reason is the MTS Si:C 1:1 ratio is the same as the Si:C ratio of the SiC product. Another reason may be that the SiC CVD using MTS as precursor molecules produces a byproduct HCl, which might play an important role in suppressing the deposition of pure Si crystal during the growth of the SiC films or crystals.[18] The H_2 carrier gas may facilitate the reduction of the Si−Cl bonds on the growing surface of SiC, thereby increasing the deposition rate.

Several important questions have yet to be answered regarding the CVD process. These include how HCl or H_2 affects the deposition rate and the quality of SiC under various reaction conditions, such as the gas-phase temperature. To improve the

10.1021/jp065453q CCC: $37.00
Published on Web 02/03/2007

TABLE 1: Point Groups and Structures of Studied Species

Isomer	Point Group	Structure [a]
1. Cl		
2. Cl_2	$D_{\infty h}$	
3. H		
4. H_2	$D_{\infty h}$	
5. HCl	$C_{\infty v}$	
6. C_2H	$C_{\infty v}$	
7. C_2H_2	$D_{\infty h}$	
8. C_2H_3	C_s	
9. C_2H_3Cl	C_s	
10. C_2H_4	D_{2h}	
11. C_2H_5	C_s	
12. C_2H_5Cl	C_s	
13. C_2H_6(e) [b]	C_{3h}	
14. C_2H_6	D_{3d}	
15. $^1CH_2$	C_{2v}	
16. $^3CH_2$	C_{2v}	
17. CH_2C	C_{2v}	
18. CH_2Cl	C_s	
19. CH_2Cl_2	C_{2v}	
20. CH_3	D_{3h}	
21. CH_3CH(s) [c]	C_s	
22. CH_3Cl	C_{3v}	
23. CH_4	T_d	
24. HCHC [d]	C_s	
25. Si_2Cl_4	C_{2h}	
26. Si_2Cl_5	C_s	
27. Si_2Cl_6	D_{3d}	
28. $SiCl_2$	C_{2v}	
29. $SiCl_3$	C_{3v}	
30. $SiCl_4$	T_d	
31. SiH_2Cl	C_s	
32. SiH_2Cl_2	C_{2v}	
33. SiH_3Cl	C_{3v}	
34. SiHCl	C_s	
35. $SiHCl_2$	C_s	
36. $SiHCl_3$	C_{3v}	
37. CH_2SiCl_2	C_{2v}	
38. CH_2SiCl_3	C_s	
39. CH_2SiHCl	C_s	
40. CH_2SiHCl_2	C_s	
41. CH_3SiCl	C_s	
42. CH_3SiCl_2	C_s	
43. CH_3SiCl_2Cl [e]	C_1	
44. CH_3SiCl_3	C_{3v}	
45. CH_3SiH_2Cl	C_s	
46. CH_3SiHCl	C_1	
47. CH_3SiHCl_2	C_s	
48. CHSiCl	C_s	
49. $^1CHSiCl_3$	C_1	
50. $^3CHSiCl_3$	C_s	

[a] Solid dark gray balls are C atoms. White balls are H atoms. Balls with blue strips are Si atoms. Balls with green dots are Cl atoms. [b] Species 13 C_2H_6(e) has an eclipsed conformation; it is a TS connecting two identical C_2H_6 with staggered conformation. [c] Species 21 CH_3CH(s) has a staggered conformation; it is a TS connecting two identical ethylenes (C_2H_4). [d] Species 24 HCHC is an intermediate between acetylene (C_2H_2) and vinylidene (CH_2C). [e] Species 43 CH_3SiCl_2Cl is an intermediate between CH_3SiCl_3 and $CH_3SiCl + Cl_2$.

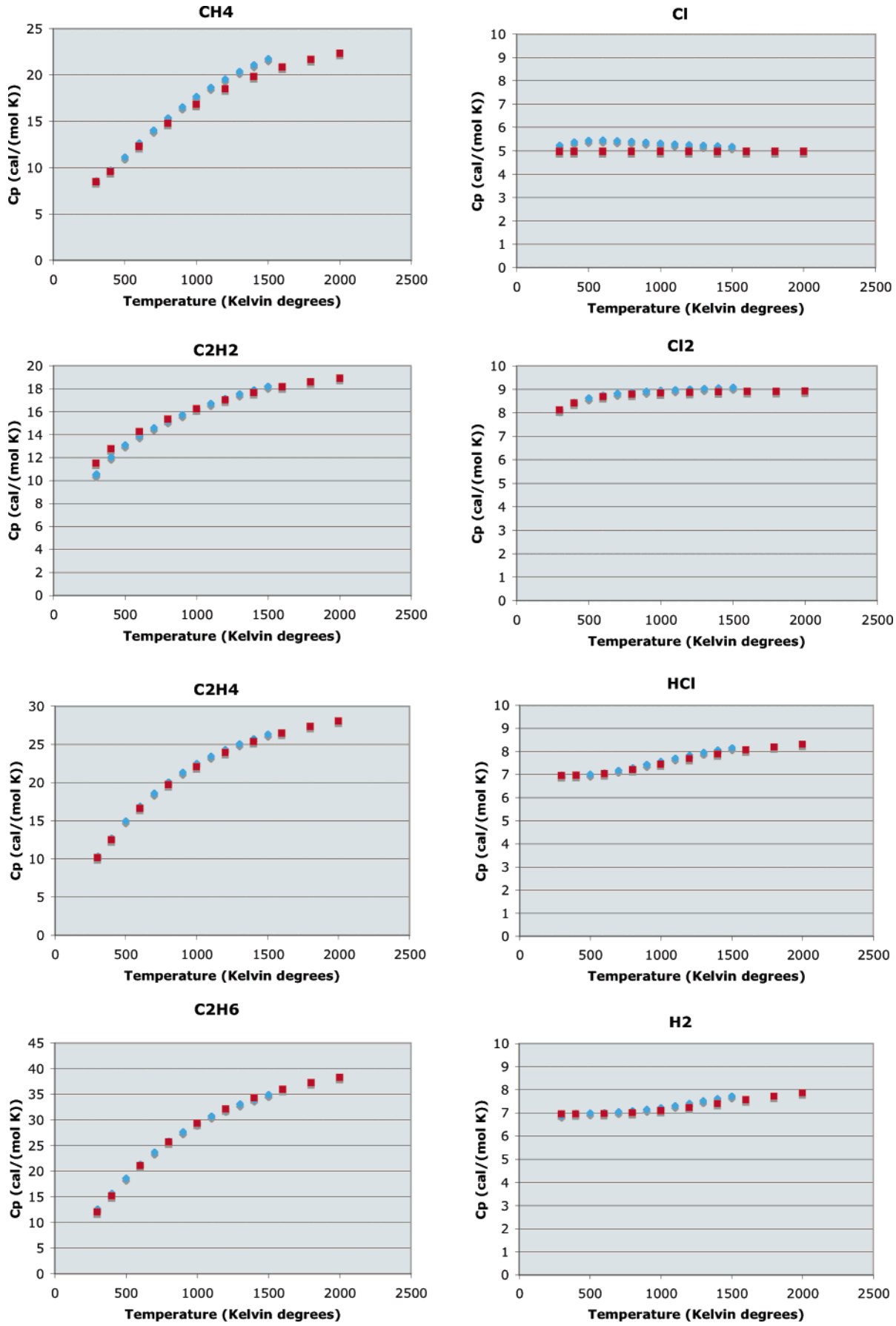

Figure 2. (Part 1 of 2).

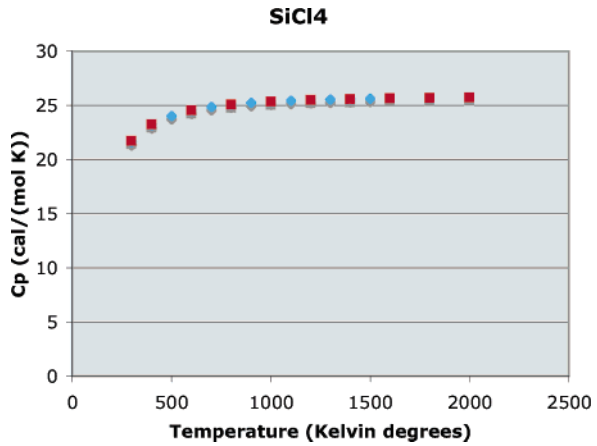

Figure 2. (Part 2 of 2). Comparison between predicted (red squares) and experimental (blue rhombus) C_p values.

CVD technique for growing high quality SiC at a reasonable deposition rate, a better understanding of the mechanism of the CVD process is needed. One challenge to unraveling the CVD mechanism is to determine how the gas-phase composition changes with residence time, temperature and other reaction conditions. Tens or even hundreds of species including various molecules, radicals, and atoms can be produced and coexist in the gas phase at various high CVD temperatures. These gas-phase species may react with each other and/or interact with the surface of the pyrolytic carbon at the initial stage of the CVD process. They can also interact with the growing SiC surface after the first layer of SiC has been formed on the pyrolytic C surface. It is desirable, but not necessarily feasible, to simplify the gas-phase reaction mechanism by excluding some species; for example, species with low concentrations or species with low chemical reactivity with the C or SiC surface. Reactive species, such as CH_3 and $SiCl_3$ radicals, that might have very low concentrations in the gas phase, often play an important role in the heterogeneous chemical reactions that account for the deposition and growth of SiC. On the other hand, some kinetically stable species that exhibit very low reactivity with the surface, such as CH_4, C_2H_6, and $SiCl_4$, often have high concentrations during the CVD process and serve as a major source for the production of active radicals such as CH_3 and $SiCl_3$. Due to the complexity of the gas-phase chemistry of SiC CVD, mechanisms proposed from kinetic modeling based on the analysis of experimental data are often incomplete or inaccurate. Thus, a careful, systematic theoretical study of the gas-phase chemistry of SiC CVD is desirable.

This paper presents a thorough study of the thermodynamic properties of various possible gas-phase species produced during the CVD that uses MTS as the precursor and H_2 as the auxiliary gas. The detailed reaction paths that lead to the production and consumption of the gas-phase species, the corresponding transition state structures and the related thermodynamic and kinetic data are presented and discussed in the following paper.

The remainder of this paper is organized as follows. In section II, the computational methods for obtaining the local minimum energy structures and thermodynamic data of the gas-phase species are briefly introduced. In section III, structures and point groups of various gas-phase species are tabulated. A 114-reaction mechanism is then proposed to account for the production and consumption of the studied gas-phase species. Reaction enthalpies, entropies, and Gibbs free energies are tabulated. Careful comparison between the calculated and experimental thermodynamic properties of various species is presented. The Supporting Information provided with this paper includes the predicted energies, zero point energies, Cartesian coordinates, and vibrational frequencies of all of the species studied in this work. Values of isobaric heat capacity at atmospheric pressure are also provided in the Supporting Information, because they are often indispensable for chemical kinetic simulations.

II. Computational Details

Geometries, energies, harmonic vibrational frequencies, and zero point energies have been obtained using restricted (for closed-shell species) and unrestricted (for open-shell species) second-order perturbation theory (MP2)[41] with the Dunning aug-cc-pVDZ basis set.[42,43] Hessian (energy second derivative) calculations were performed to obtain thermodynamic properties. MP2 single-point energies were obtained at these geometries, with the triple-ζ aug-cc-pVTZ basis set.[42,43] Coupled cluster with single and double excitations and perturbative triples (CCSD(T))/aug-cc-pVDZ single point energy calculations were also performed at the MP2/aug-cc-pVDZ geometries. CCSD(T)/aug-cc-pVTZ single point energies were estimated by assuming the additivity of correlation and basis set corrections:

$$E_{\mathrm{CCSD(T)/aug-cc-pVTZ}} \approx E_{\mathrm{CCSD(T)/aug-cc-pVDZ}} + (E_{\mathrm{MP2/aug-cc-pVTZ}} - E_{\mathrm{MP2/aug-cc-pVDZ}}) \quad (1)$$

Comparison between the estimated and true CCSD(T)/aug-cc-pVTZ energies were made for small molecules including $^1CH_2$, $^3CH_2$, CH_3, CH_4, C_2H_x ($x = 1-6$), H_2, Cl, Cl_2, SiHCl, $SiCl_2$, SiH_2Cl. The discrepancies between the estimated and true CCSD(T) values are within ca. 0.001 hartree when no Cl atoms are present. The estimated CCSD(T)/aug-cc-pVTZ energy is about 0.008 hartree per Cl atom higher than the correct CCSD(T) result for Cl-containing species. For example, the estimated CCSD(T)/aug-cc-pVTZ energies of Cl, Cl_2, SiHCl, $SiCl_2$, SiH_2Cl are 0.0088, 0.0158, 0.0077, 0.00163, and 0.0083 hartree higher than the true CCSD(T)/aug-cc-pVTZ results, respectively. Fortunately, most of this discrepancy cancels because relative energies, not absolute energies, are of interest.

All of the MP2 calculations were done with the GAMESS suite of codes.[44] CCSD(T)/aug-cc-pVDZ singlet point calculations were performed using the ACES package.[45] Structures and vibrational frequencies were visualized with the aid of MacMolPlt.[46]

III. Results and Discussion

Table 1 illustrates the structures and point groups of the studied gas-phase species that are produced during and after the chemical vapor deposition of silicon carbide with MTS and H_2 as precursor molecules. All species with an even (odd) number of electrons is a singlet (doublet) state unless noted otherwise. The thermodynamic properties of all Cl-containing species were calculated with assumption of the presence of only ^{35}Cl isotopes. Some species, such as CH_3SiCl and $^1CHSiCl_3$ with C_1 symmetry, can have two enantiomers, but this has no effect on any computed energetic properties.

Predicted thermodynamic properties may be compared with experimental values from the *CRC Handbook*[40] for CH_4, C_2H_2, C_2H_4, C_2H_6, Cl, Cl_2, HCl, H, H_2, and $SiCl_4$ in the gas phase at various temperatures ranging from 298.15 to 1400 K. Figure 2 shows that the theoretical and experimental isobaric (at 1 atm) heat capacities agree well for all of these species at all temperatures.[47] The discrepancies between the theoretical and experimental C_p values are generally less than 0.5 cal/(mol K). The largest C_p discrepancy is 1.3 cal/(mol K) for CH_4 at 1400

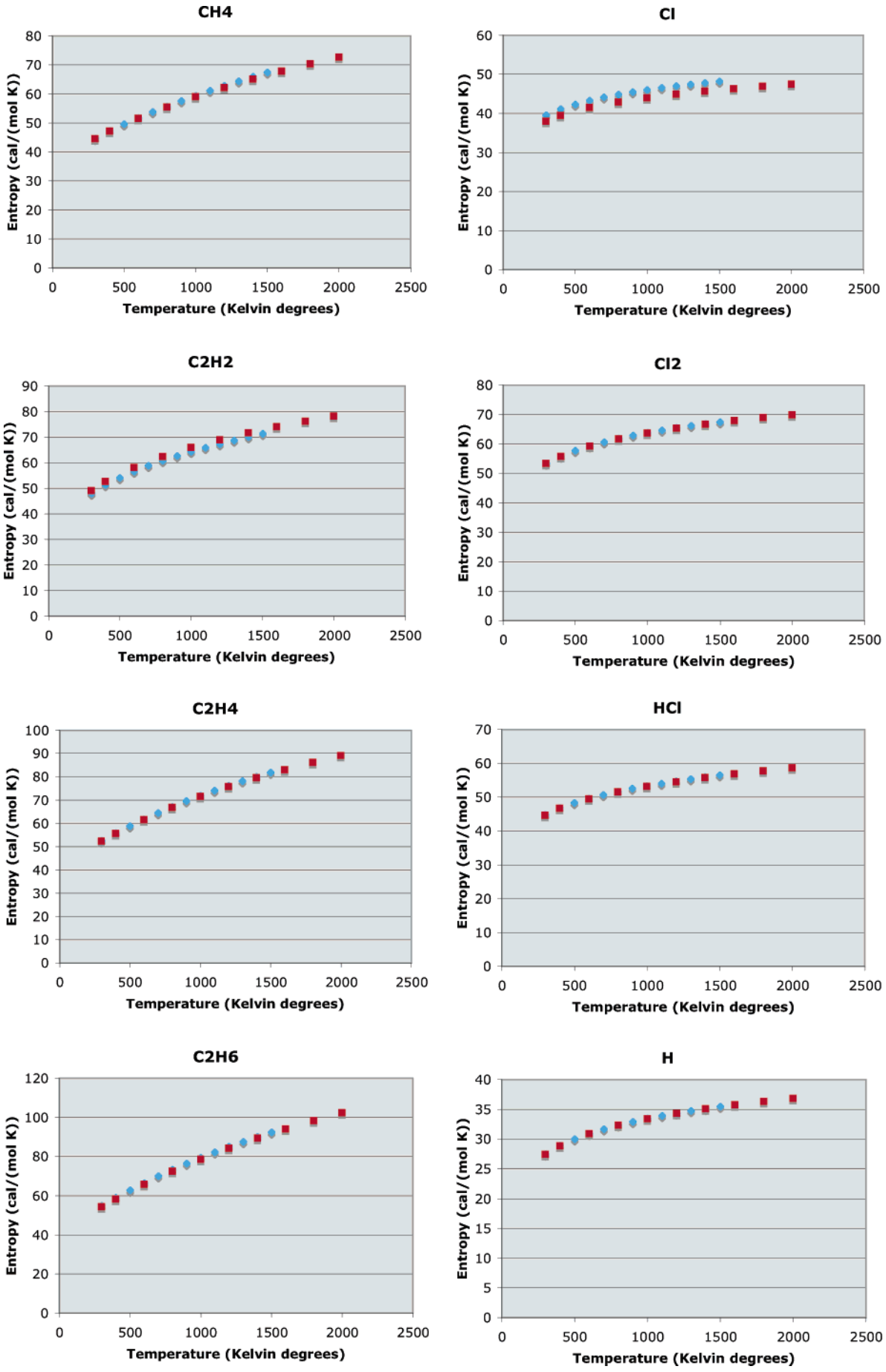

Figure 3. (Part 1 of 2).

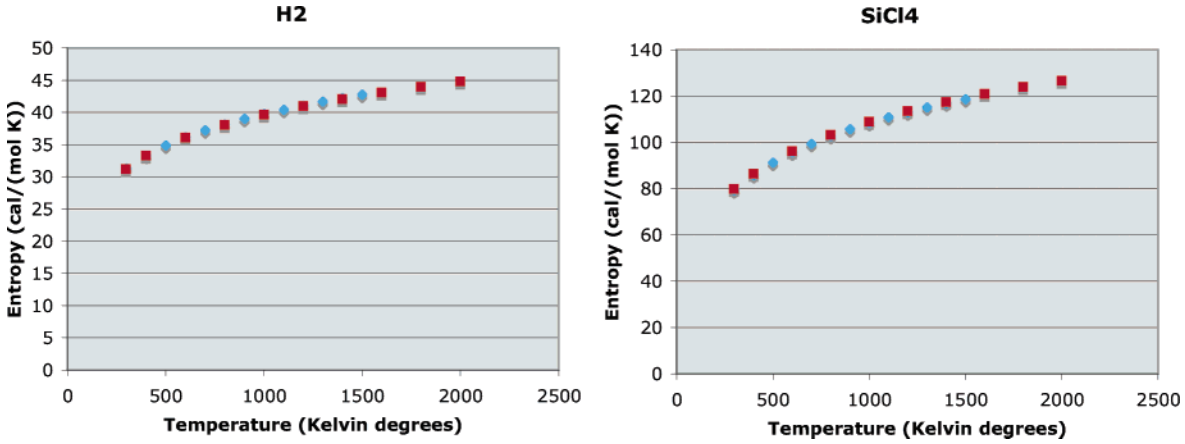

Figure 3. (Part 2 of 2). Comparison between predicted (red squares) and experimental (blue rhombus) entropy values.

TABLE 2: Enthalpy Changes (kcal/mol) of the Decomposition Reactions of CH_3SiCl_3 and Consecutive Reactions in the Gas Phase at Various Temperatures

reaction	0 K	298.15 K	400 K	600 K	800 K	1000 K	1200 K	1400 K	1600 K	1800 K	2000 K
1. $CH_3SiCl_3 \rightarrow CH_3 + SiCl_3$	91.6	92.9	93.0	92.9	92.5	91.9	91.3	90.6	89.8	89.1	88.3
2. $CH_3SiCl_3 \rightarrow H + CH_2SiCl_3$	101.1	102.8	103.3	104.1	104.7	105.1	105.4	105.6	105.7	105.7	105.7
3. $CH_3SiCl_3 \rightarrow Cl + CH_3SiCl_2$	108.4	109.1	109.1	109.1	109.0	108.8	108.7	108.5	108.3	108.1	107.9
4. $CH_3SiCl_3 \rightarrow CH_2SiCl_2 + HCl$	78.8	79.8	79.9	79.9	79.8	79.4	79.0	78.6	78.1	77.5	77.0
5. $CH_3SiCl_3 \rightarrow CH_3Cl + SiCl_2$	72.6	73.0	72.7	71.9	71.1	70.3	69.4	68.6	67.8	67.0	66.1
6. $CH_3SiCl_3 \rightarrow {}^1CH_2 + SiHCl_3$	118.2	119.4	119.5	119.5	119.2	118.8	118.3	117.8	117.2	116.6	115.9
7. $CH_3SiCl_3 \rightarrow {}^1CHSiCl_3 + H_2$	119.7	121.4	121.9	122.5	122.8	122.9	122.8	122.5	122.2	121.8	121.4
8. $CH_3SiCl_3 \rightarrow CH_3SiCl + Cl_2$	128.3	129.0	128.9	128.6	128.2	127.7	127.1	126.6	126.1	125.5	124.9
9. $H_2 \rightarrow H + H$	102.8	103.6	103.9	104.5	105.1	105.7	106.3	106.8	107.3	107.7	108.2
10. $HCl \rightarrow H + Cl$	101.2	102.1	102.4	103.0	103.6	104.1	104.6	105.0	105.4	105.8	106.1
11. $Cl_2 \rightarrow Cl + Cl$	53.8	54.6	54.8	55.0	55.3	55.5	55.7	55.9	56.1	56.3	56.5
12. $Cl + H_2 \rightarrow HCl + H$	1.5	1.5	1.5	1.5	1.5	1.6	1.7	1.8	1.9	2.0	2.1
13. $Cl + HCl \rightarrow Cl_2 + H$	47.4	47.5	47.7	48.0	48.3	48.6	48.9	49.1	49.3	49.4	49.6
14. $CH_3 + H_2 \rightarrow CH_4 + H$	0.5	−0.2	−0.5	−0.9	−1.0	−0.9	−0.7	−0.4	−0.1	0.3	0.7
15. $CH_3 + H \rightarrow {}^3CH_2 + H_2$	5.0	5.5	5.6	5.6	5.4	5.2	4.9	4.5	4.1	3.7	3.3
16. $CH_3 + H \rightarrow CH_4$	−102.3	−103.9	−104.5	−105.4	−106.1	−106.6	−107.0	−107.2	−107.3	−107.4	−107.4
17. $CH_3 + CH_3 \rightarrow C_2H_6$	−86.6	−88.8	−89.4	−90.1	−90.3	−90.1	−89.7	−89.2	−88.6	−87.9	−87.2
18. $CH_3 + CH_3 \rightarrow C_2H_5 + H$	12.4	11.9	11.9	12.1	12.6	13.3	14.0	14.8	15.5	16.2	16.9
19. $CH_3 + CH_3 \rightarrow {}^3CH_2 + CH_4$	5.5	5.3	5.0	4.7	4.4	4.2	4.1	4.1	4.0	4.0	4.0
20. $CH_3 \rightarrow {}^3CH_2 + H$	107.8	109.1	109.5	110.1	110.6	110.9	111.1	111.3	111.4	111.4	111.4
21. $CH_3 + HCl \rightarrow CH_3Cl + H$	20.5	19.9	19.7	19.8	20.1	20.5	20.9	21.4	21.9	22.4	22.9
22. $CH_3 + HCl \rightarrow CH_4 + Cl$	−1.0	−1.8	−2.0	−2.4	−2.6	−2.5	−2.4	−2.2	−1.9	−1.6	−1.3
23. $CH_3Cl + H_2 \rightarrow CH_4 + HCl$	−20.0	−20.1	−20.3	−20.7	−21.1	−21.4	−21.7	−21.8	−22.0	−22.1	−22.1
24. $CH_2Cl + HCl \rightarrow CH_2Cl_2 + H$	24.0	23.6	23.6	23.8	24.2	24.7	25.2	25.7	26.2	26.7	27.2
25. ${}^3CH_2 + CH_3 \rightarrow C_2H_5$	−95.4	−97.3	−97.6	−98.0	−97.9	−97.6	−97.1	−96.5	−95.9	−95.2	−94.5
26. ${}^3CH_2 + CH_3 \rightarrow C_2H_4 + H$	−60.3	−61.2	−61.4	−61.4	−61.1	−60.6	−60.0	−59.4	−58.7	−58.1	−57.4
27. ${}^3CH_2 + {}^3CH_2 \rightarrow C_2H_2 + H + H$	−25.4	−24.6	−24.0	−22.9	−21.7	−20.6	−19.5	−18.5	−17.6	−16.7	−15.8
28. ${}^3CH_2 + {}^3CH_2 \rightarrow C_2H_2 + H_2$	−128.1	−128.2	−128.0	−127.4	−126.8	−126.3	−125.8	−125.3	−124.8	−124.4	−124.0
29. $C_2H_6 \rightarrow C_2H_5 + H$	98.9	100.7	101.3	102.2	102.9	103.4	103.7	103.9	104.1	104.1	104.1
30. $C_2H_6 \rightarrow C_2H_4 + H_2$	31.3	33.1	33.5	34.2	34.6	34.7	34.5	34.3	33.9	33.5	33.1
31. $C_2H_6 \rightarrow C_2H_6(e)$	2.5	2.2	2.0	1.6	1.2	0.8	0.4	0.0	−0.4	−0.8	−1.2
32. $C_2H_6(e) \rightarrow C_2H_4 + H_2$	28.8	30.9	31.5	32.6	33.3	33.8	34.1	34.2	34.3	34.3	34.2
33. $C_2H_6 + H \rightarrow C_2H_5 + H_2$	−3.8	−2.9	−2.7	−2.3	−2.2	−2.3	−2.6	−2.9	−3.2	−3.6	−4.0
34. $C_2H_5 \rightarrow C_2H_4 + H$	35.1	36.0	36.2	36.5	36.8	37.0	37.1	37.2	37.2	37.1	37.1
35. $C_2H_5 + H \rightarrow C_2H_4 + H_2$	−67.7	−67.6	−67.7	−68.0	−68.3	−68.7	−69.2	−69.6	−70.1	−70.6	−71.1
36. $C_2H_4 \rightarrow C_2H_3 + H$	109.9	111.4	111.9	112.6	113.0	113.4	113.6	113.8	113.9	113.9	113.9
37. $C_2H_4 \rightarrow CH_2C + H_2$	82.1	84.4	85.1	86.1	86.5	86.7	86.7	86.6	86.3	86.0	85.6
38. $CH_2C \rightarrow HCHC$	1.3	1.2	1.2	1.2	1.2	1.3	1.3	1.4	1.4	1.5	1.5
39. $HCHC \rightarrow C_2H_2$	−43.5	−43.5	−43.4	−43.1	−42.9	−42.8	−42.7	−42.6	−42.5	−42.3	−42.2
40. $C_2H_6 \rightarrow CH_3CH(s) + H_2$	104.4	106.2	106.7	107.2	107.4	107.2	106.8	106.3	105.7	105.0	104.2
41. $C_2H_4 \rightarrow CH_3CH(s)$	73.2	73.2	73.1	73.0	72.8	72.6	72.3	72.0	71.8	71.4	71.1
42. $CH_3CH(s) \rightarrow C_2H_2 + H_2$	−33.2	−31.0	−30.2	−28.9	−28.0	−27.3	−26.9	−26.7	−26.5	−26.4	−26.3
43. $C_2H_4 + H \rightarrow C_2H_3 + H_2$	7.2	7.8	7.9	8.0	7.9	7.7	7.4	7.0	6.6	6.2	5.7
44. $C_2H_3 \rightarrow C_2H_2 + H$	32.8	34.4	35.0	36.1	36.9	37.5	38.0	38.4	38.7	38.9	39.1
45. $C_2H_3 + H \rightarrow C_2H_2 + H_2$	−69.9	−69.3	−68.9	−68.4	−68.2	−68.2	−68.3	−68.4	−68.6	−68.8	−69.1
46. $C_2H_3 + CH_4 \rightarrow C_2H_4 + CH_3$	−7.7	−7.5	−7.4	−7.1	−6.9	−6.8	−6.6	−6.6	−6.5	−6.5	−6.5
47. $C_2H_3 + C_2H_6 \rightarrow C_2H_4 + C_2H_5$	−11.0	−10.7	−10.6	−10.3	−10.1	−10.0	−9.9	−9.9	−9.8	−9.8	−9.8
48. $C_2H_3 + C_2H_5 \rightarrow C_2H_4 + C_2H_4$	−74.9	−75.4	−75.7	−76.0	−76.2	−76.4	−76.5	−76.6	−76.7	−76.8	−76.8
49. $C_2H_2 + H \rightarrow C_2H + H_2$	31.8	32.0	31.9	31.5	31.1	30.6	30.1	29.6	29.1	28.6	28.1
50. $C_2H_6 + CH_3 \rightarrow C_2H_5 + CH_4$	−3.3	−3.2	−3.2	−3.2	−3.2	−3.3	−3.3	−3.3	−3.3	−3.3	−3.3
51. $C_2H_6 + {}^3CH_2 \rightarrow C_2H_5 + CH_3$	−8.8	−8.4	−8.2	−7.9	−7.6	−7.5	−7.4	−7.4	−7.3	−7.3	−7.3

TABLE 2 (Continued)

reactions	0 K	298.15 K	400 K	600 K	800 K	1000 K	1200 K	1400 K	1600 K	1800 K	2000 K
52. $C_2H_4 + HCl \rightarrow C_2H_5Cl$	−16.3	−17.8	−18.0	−18.2	−18.0	−17.8	−17.4	−16.9	−16.4	−15.9	−15.4
53. $C_2H_2 + HCl \rightarrow C_2H_3Cl$	−25.1	−27.0	−27.5	−28.1	−28.3	−28.3	−28.2	−28.0	−27.7	−27.4	−27.1
54. $C_2H_5 + HCl \rightarrow C_2H_5Cl + H$	18.7	18.2	18.2	18.4	18.8	19.2	19.7	20.2	20.7	21.2	21.7
55. $C_2H_5 + HCl \rightarrow C_2H_6 + Cl$	2.3	1.4	1.1	0.8	0.7	0.7	0.9	1.1	1.4	1.6	2.0
56. $C_2H_3 + HCl \rightarrow C_2H_3Cl + H$	7.7	7.4	7.6	8.0	8.6	9.2	9.8	10.4	11.0	11.5	12.0
57. $C_2H_3 + HCl \rightarrow C_2H_4 + Cl$	−8.7	−9.3	−9.4	−9.5	−9.5	−9.3	−9.0	−8.8	−8.5	−8.1	−7.8
58. $^3CH_2 + HCl \rightarrow CH_3 + Cl$	−6.6	−7.0	−7.1	−7.1	−7.0	−6.8	−6.5	−6.3	−6.0	−5.7	−5.3
59. $^3CH_2 + HCl \rightarrow CH_2Cl + H$	10.6	10.3	10.4	10.7	11.2	11.8	12.3	12.8	13.4	13.9	14.3
60. $SiCl_3 + SiCl_3 \rightarrow SiCl_2 + SiCl_4$	−43.8	−43.8	−43.8	−43.8	−43.8	−43.8	−43.8	−43.8	−43.8	−43.8	−43.8
61. $SiCl_2 + SiCl_3 \rightarrow Si_2Cl_5$	−34.2	−34.0	−33.7	−33.0	−32.2	−31.5	−30.7	−29.9	−29.1	−28.3	−27.6
62. $SiCl_2 + SiCl_2 \rightarrow Si_2Cl_4$	−12.9	−12.7	−12.3	−11.6	−10.8	−10.1	−9.3	−8.5	−7.7	−6.9	−6.1
63. $SiCl_3 + SiCl_3 \rightarrow Si_2Cl_6$	−76.4	−76.2	−75.9	−75.2	−74.4	−73.7	−72.9	−72.1	−71.4	−70.6	−69.8
64. $SiCl_2 + SiCl_4 \rightarrow Si_2Cl_6$	−32.7	−32.4	−32.1	−31.4	−30.7	−29.9	−29.1	−28.4	−27.6	−26.8	−26.0
65. $SiCl_3 \rightarrow SiCl_2 + Cl$	61.7	62.4	62.4	62.3	62.1	62.0	61.8	61.6	61.4	61.2	61.1
66. $SiCl_4 \rightarrow SiCl_3 + Cl$	105.5	106.1	106.1	106.0	105.9	105.7	105.6	105.4	105.2	105.0	104.8
67. $SiCl_4 + H_2 \rightarrow SiHCl_3 + HCl$	17.0	16.2	15.9	15.4	15.0	14.7	14.5	14.4	14.3	14.3	14.3
68. $SiCl_3 + H_2 \rightarrow SiHCl_3 + H$	12.8	12.2	12.2	12.3	12.6	13.1	13.5	14.0	14.5	15.1	15.6
69. $SiCl_3 + H_2 \rightarrow SiHCl_2 + HCl$	18.2	17.5	17.2	16.7	16.3	16.1	15.9	15.8	15.8	15.8	15.8
70. $SiCl_3 + HCl \rightarrow SiCl_4 + H$	−4.3	−4.0	−3.7	−3.0	−2.3	−1.6	−1.0	−0.4	0.2	0.7	1.3
71. $SiCl_3 + HCl \rightarrow SiHCl_3 + Cl$	11.3	10.7	10.7	10.8	11.1	11.5	11.8	12.3	12.7	13.1	13.5
72. $SiCl_2 + H_2 \rightarrow SiH_2Cl_2$	−31.9	−33.8	−34.1	−34.4	−34.4	−34.2	−33.7	−33.3	−32.7	−32.1	−31.5
73. $SiCl_2 + H_2 \rightarrow SiHCl + HCl$	29.7	29.3	29.0	28.6	28.3	28.1	28.0	27.9	27.9	27.9	27.9
74. $SiCl_2 + H_2 \rightarrow SiHCl_2 + H$	57.7	57.2	57.2	57.4	57.8	58.2	58.7	59.2	59.8	60.3	60.8
75. $SiCl_2 + HCl \rightarrow SiCl_3 + H$	39.5	39.8	40.1	40.7	41.4	42.1	42.8	43.4	44.0	44.5	45.0
76. $SiCl_2 + HCl \rightarrow SiHCl_2 + Cl$	56.2	55.7	55.7	55.9	56.2	56.6	57.0	57.5	57.9	58.3	58.8
77. $SiHCl_3 \rightarrow SiCl_2 + HCl$	50.4	51.6	51.7	51.5	51.0	50.5	50.0	49.4	48.8	48.2	47.5
78. $SiHCl_3 \rightarrow SiCl_3 + H$	90.0	91.4	91.7	92.2	92.5	92.7	92.7	92.8	92.7	92.7	92.6
79. $SiHCl_2 \rightarrow SiCl_2 + H$	45.0	46.4	46.7	47.1	47.4	47.5	47.6	47.6	47.5	47.4	47.4
80. $SiHCl_3 \rightarrow SiHCl_2 + Cl$	106.7	107.4	107.4	107.4	107.3	107.1	107.0	106.8	106.7	106.5	106.3
81. $SiH_2Cl_2 \rightarrow SiHCl_2 + H$	89.6	91.0	91.4	91.9	92.2	92.4	92.5	92.5	92.5	92.4	92.3
82. $SiH_2Cl_2 \rightarrow SiH_2Cl + Cl$	106.3	107.2	107.3	107.3	107.3	107.2	107.0	106.9	106.7	106.6	106.4
83. $SiH_2Cl_2 \rightarrow SiHCl + HCl$	61.6	63.0	63.2	63.0	62.7	62.3	61.7	61.2	60.6	60.0	59.4
84. $SiHCl_3 + H_2 \rightarrow SiH_2Cl_2 + HCl$	18.6	17.9	17.5	17.0	16.6	16.4	16.2	16.1	16.1	16.0	16.0
85. $SiHCl_2 + H_2 \rightarrow SiH_2Cl_2 + H$	13.1	12.6	12.6	12.7	13.0	13.4	13.8	14.3	14.8	15.3	15.8
86. $SiHCl_2 + HCl \rightarrow SiHCl_3 + H$	−5.4	−5.2	−5.0	−4.3	−3.7	−3.0	−2.4	−1.8	−1.2	−0.7	−0.2
87. $SiHCl_2 + HCl \rightarrow SiH_2Cl_2 + Cl$	11.6	11.1	11.1	11.2	11.4	11.8	12.1	12.5	12.9	13.4	13.8
88. $SiHCl + H_2 \rightarrow SiH_3Cl$	−43.4	−45.2	−45.6	−46.0	−46.0	−45.8	−45.5	−45.0	−44.5	−43.9	−43.3
89. $SiHCl + HCl \rightarrow SiHCl_2 + H$	28.0	28.0	28.2	28.8	29.5	30.1	30.7	31.3	31.9	32.4	32.9
90. $SiHCl + HCl \rightarrow SiH_2Cl + Cl$	44.6	44.1	44.1	44.3	44.6	44.9	45.3	45.7	46.1	46.6	47.0
91. $SiCl_3 + CH_4 \rightarrow CH_3SiCl_3 + H$	10.6	10.9	11.4	12.6	13.7	14.7	15.7	16.6	17.5	18.3	19.1
92. $SiCl_3 + CH_4 \rightarrow SiHCl_3 + CH_3$	12.3	12.5	12.7	13.2	13.6	14.0	14.2	14.4	14.6	14.7	14.8
93. $SiCl_3 + CH_3 \rightarrow SiCl_2 + CH_3Cl$	−19.0	−19.9	−20.3	−21.0	−21.4	−21.7	−21.8	−22.0	−22.1	−22.1	−22.2
94. $SiCl_3 + CH_3 \rightarrow SiHCl_3 + {}^3CH_2$	17.8	17.7	17.8	17.9	18.1	18.2	18.4	18.5	18.6	18.7	18.8
95. $SiCl_2 + CH_4 \rightarrow CH_3SiHCl_2$	−33.0	−34.0	−33.9	−33.2	−32.3	−31.5	−30.5	−29.6	−28.7	−27.8	−27.0
96. $SiCl_2 + CH_4 \rightarrow SiHCl_2 + CH_3$	57.2	57.5	57.8	58.3	58.8	59.1	59.4	59.6	59.8	60.0	60.1
97. $CH_2SiCl_2 + H_2 \rightarrow CH_3SiHCl_2$	−59.2	−60.9	−61.4	−61.9	−62.1	−62.0	−61.8	−61.4	−61.0	−60.5	−60.0
98. $CH_3SiHCl_2 \rightarrow CH_2SiHCl + HCl$	74.2	75.3	75.5	75.5	75.3	75.0	74.6	74.2	73.7	73.2	72.6
99. $CH_3SiCl_2 + H_2 \rightarrow CH_3SiHCl_2 + H$	12.4	11.9	11.9	12.0	12.3	12.7	13.2	13.7	14.2	14.7	15.2
100. $CH_2SiCl_3 + H_2 \rightarrow CH_3SiCl_3 + H$	1.7	0.8	0.6	0.4	0.4	0.6	0.9	1.2	1.6	2.0	2.5
101. $CH_3 + CH_3SiCl_3 \rightarrow CH_4 + CH_2SiCl_3$	−1.2	−1.1	−1.2	−1.3	−1.4	−1.5	−1.6	−1.6	−1.7	−1.7	−1.7
102. $CH_3 + CH_3SiCl_3 \rightarrow CH_3Cl + CH_3SiCl_2$	27.7	26.9	26.5	25.8	25.4	25.2	25.0	24.9	24.8	24.8	24.7
103. $SiCl_3 + CH_3SiCl_3 \rightarrow SiHCl_3 + CH_2SiCl_3$	11.1	11.4	11.6	11.9	12.2	12.5	12.6	12.8	12.9	13.0	13.1
104. $SiCl_3 + CH_3SiCl_3 \rightarrow SiCl_4 + CH_3SiCl_2$	3.0	3.0	3.0	3.0	3.1	3.1	3.1	3.1	3.1	3.1	3.1
105. $H + CH_3SiCl_3 \rightarrow HCl + CH_3SiCl_2$	7.2	7.0	6.7	6.1	5.4	4.7	4.1	3.5	2.9	2.4	1.8
106. $Cl + CH_3SiCl_3 \rightarrow HCl + CH_2SiCl_3$	−0.1	0.7	0.9	1.1	1.1	1.0	0.8	0.5	0.3	−0.1	−0.4
107. $CH_2SiCl_3 \rightarrow {}^3CH_2 + SiCl_3$	98.3	99.3	99.2	98.9	98.3	97.7	97.0	96.3	95.6	94.8	94.0
108. $CH_2SiCl_3 \rightarrow CH_2SiCl_2 + Cl$	79.0	79.2	79.1	78.8	78.6	78.4	78.2	78.0	77.8	77.6	77.4
109. $CH_3SiCl_2 \rightarrow CH_3 + SiCl_2$	44.9	46.2	46.2	46.1	45.6	45.1	44.4	43.7	43.0	42.2	41.4
110. $CH_3SiCl_2 \rightarrow H + CH_2SiCl_2$	71.6	72.8	73.2	73.9	74.4	74.7	74.9	75.1	75.2	75.2	75.2
111. $CH_3SiCl_3 \rightarrow CH_3SiCl_2Cl$	111.1	111.5	111.6	111.7	111.7	111.7	111.7	111.8	111.8	111.8	111.8
112. $CH_3SiCl_2Cl \rightarrow CH_3SiCl + Cl_2$	17.2	17.5	17.3	16.9	16.4	15.9	15.4	14.9	14.3	13.7	13.2
113. $CH_3SiCl + H_2 \rightarrow CH_3SiH_2Cl$	−42.5	−44.4	−44.8	−45.2	−45.2	−45.0	−44.6	−44.2	−43.6	−43.1	−42.5
114. $CH_3SiCl + HCl \rightarrow CH_3SiHCl_2$	−62.8	−64.1	−64.2	−64.1	−63.7	−63.3	−62.7	−62.2	−61.6	−61.0	−60.4

K. Figure 3 shows that the calculated entropies also agree well with the experimental values. Most entropy discrepancies are less than 0.5 cal/(mol K); the largest discrepancy is 2.1 cal/(mol K) for the Cl atom at 1400 K.

As noted earlier, it is difficult to propose a mechanism for the gas-phase chemistry involving MTS as precursor and H_2 as carrier gas at high CVD temperatures. Stable species usually have lower reactivity; however, they may serve as a major source of highly reactive species. Therefore, various strategies were applied to make a reaction list to account for the gas-phase chemistry. One strategy is to review available experimental data to decide what species have high concentrations in the gas phase. Gas chromatography experiments by Zhang and Huttinger suggest that the major species with significant concentration in the gas phase are H_2, CH_4, $SiCl_4$, HCl, $SiHCl_3$, and CH_3SiCl_3.[22] CH_4, CH_3Cl, $SiCl_2$, and CH_2SiCl_2 were detected

TABLE 3: Entropy Changes (cal/(mol K)) of the Decomposition Reactions of CH_3SiCl_3 and Consecutive Reactions in the Gas Phase at Various Temperatures

reaction	0 K	298.15 K	400 K	600 K	800 K	1000 K	1200 K	1400 K	1600 K	1800 K	2000 K
1. $CH_3SiCl_3 \rightarrow CH_3 + SiCl_3$	0.0	39.8	40.1	39.8	39.2	38.6	38.0	37.5	37.0	36.5	36.1
2. $CH_3SiCl_3 \rightarrow H + CH_2SiCl_3$	0.0	33.9	35.3	37.0	37.9	38.3	38.6	38.7	38.8	38.8	38.8
3. $CH_3SiCl_3 \rightarrow Cl + CH_3SiCl_2$	0.0	34.5	34.6	34.5	34.3	34.1	34.0	33.9	33.7	33.6	33.5
4. $CH_3SiCl_3 \rightarrow CH_2SiCl_2 + HCl$	0.0	36.3	36.6	36.6	36.4	36.0	35.6	35.3	34.9	34.6	34.4
5. $CH_3SiCl_3 \rightarrow CH_3Cl + SiCl_2$	0.0	40.0	39.0	37.5	36.3	35.3	34.6	34.0	33.4	32.9	32.5
6. $CH_3SiCl_3 \rightarrow {}^1CH_2 + SiHCl_3$	0.0	37.1	37.4	37.3	36.9	36.4	36.0	35.6	35.2	34.8	34.5
7. $CH_3SiCl_3 \rightarrow {}^1CHSiCl_3 + H_2$	0.0	31.8	33.0	34.3	34.8	34.9	34.8	34.6	34.4	34.1	33.9
8. $CH_3SiCl_3 \rightarrow CH_3SiCl + Cl_2$	0.0	41.2	40.9	40.3	39.6	39.1	38.6	38.2	37.8	37.5	37.2
9. $H_2 \rightarrow H + H$	0.0	23.6	24.5	25.7	26.5	27.2	27.7	28.1	28.4	28.7	28.9
10. $HCl \rightarrow H + Cl$	0.0	20.7	21.6	22.8	23.6	24.2	24.7	25.0	25.2	25.5	25.6
11. $Cl_2 \rightarrow Cl + Cl$	0.0	22.6	23.1	23.6	24.0	24.2	24.4	24.6	24.7	24.9	25.0
12. $Cl + H_2 \rightarrow HCl + H$	0.0	2.8	2.8	2.9	2.9	3.0	3.0	3.1	3.2	3.2	3.3
13. $Cl + HCl \rightarrow Cl_2 + H$	0.0	−1.9	−1.5	−0.8	−0.4	0.0	0.2	0.4	0.5	0.6	0.7
14. $CH_3 + H_2 \rightarrow CH_4 + H$	0.0	−5.9	−6.7	−7.5	−7.7	−7.6	−7.4	−7.1	−6.9	−6.7	−6.5
15. $CH_3 + H \rightarrow {}^3CH_2 + H_2$	0.0	3.9	4.1	4.1	3.9	3.7	3.4	3.1	2.8	2.6	2.4
16. $CH_3 + H \rightarrow CH_4$	0.0	−29.5	−31.2	−33.2	−34.2	−34.7	−35.0	−35.2	−35.3	−35.4	−35.4
17. $CH_3 + CH_3 \rightarrow C_2H_6$	0.0	−38.8	−40.6	−42.0	−42.2	−42.0	−41.7	−41.3	−40.9	−40.5	−40.1
18. $CH_3 + CH_3 \rightarrow C_2H_5 + H$	0.0	−5.0	−5.1	−4.6	−3.8	−3.1	−2.5	−1.9	−1.4	−1.0	−0.6
19. $CH_3 + CH_3 \rightarrow {}^3CH_2 + CH_4$	0.0	−2.0	−2.6	−3.4	−3.7	−3.9	−4.0	−4.0	−4.1	−4.1	−4.1
20. $CH_3 \rightarrow {}^3CH_2 + H$	0.0	27.5	28.6	29.8	30.5	30.8	31.1	31.2	31.2	31.3	31.3
21. $CH_3 + HCl \rightarrow CH_3Cl + H$	0.0	−7.9	−8.2	−8.2	−7.8	−7.3	−6.9	−6.5	−6.2	−5.9	−5.7
22. $CH_3 + HCl \rightarrow CH_4 + Cl$	0.0	−8.7	−9.5	−10.3	−10.5	−10.5	−10.4	−10.2	−10.1	−9.9	−9.7
23. $CH_3Cl + H_2 \rightarrow CH_4 + HCl$	0.0	2.0	1.5	0.7	0.1	−0.3	−0.5	−0.6	−0.7	−0.8	−0.8
24. $CH_2Cl + HCl \rightarrow CH_2Cl_2 + H$	0.0	−12.6	−12.6	−12.2	−11.6	−11.0	−10.6	−10.2	−9.8	−9.5	−9.3
25. $^3CH_2 + CH_3 \rightarrow C_2H_5$	0.0	−32.5	−33.7	−34.4	−34.3	−33.9	−33.5	−33.1	−32.6	−32.2	−31.9
26. $^3CH_2 + CH_3 \rightarrow C_2H_4 + H$	0.0	−13.6	−14.1	−14.1	−13.7	−13.1	−12.6	−12.1	−11.7	−11.3	−10.9
27. $^3CH_2 + {}^3CH_2 \rightarrow C_2H_2 + H + H$	0.0	10.4	12.0	14.4	16.1	17.3	18.3	19.1	19.7	20.2	20.7
28. $^3CH_2 + {}^3CH_2 \rightarrow C_2H_2 + H_2$	0.0	−13.2	−12.4	−11.3	−10.4	−9.8	−9.4	−9.0	−8.7	−8.5	−8.2
29. $C_2H_6 \rightarrow C_2H_5 + H$	0.0	33.8	35.5	37.4	38.4	38.9	39.2	39.4	39.5	39.5	39.5
30. $C_2H_6 \rightarrow C_2H_4 + H_2$	0.0	29.2	30.6	32.0	32.5	32.6	32.5	32.3	32.1	31.8	31.6
31. $C_2H_6 \rightarrow C_2H_6(e)$	0.0	0.0	−0.5	−1.3	−1.9	−2.3	−2.7	−3.0	−3.3	−3.5	−3.7
32. $C_2H_6(e) \rightarrow C_2H_4 + H_2$	0.0	29.2	31.1	33.3	34.4	34.9	35.2	35.3	35.3	35.3	35.3
33. $C_2H_6 + H \rightarrow C_2H_5 + H_2$	0.0	10.2	11.0	11.8	11.9	11.8	11.6	11.3	11.1	10.9	10.6
34. $C_2H_5 \rightarrow C_2H_4 + H$	0.0	19.0	19.6	20.2	20.6	20.8	20.9	21.0	21.0	21.0	20.9
35. $C_2H_5 + H \rightarrow C_2H_4 + H_2$	0.0	−4.6	−4.9	−5.4	−5.9	−6.3	−6.7	−7.1	−7.4	−7.7	−8.0
36. $C_2H_4 \rightarrow C_2H_3 + H$	0.0	30.6	31.9	33.4	34.1	34.5	34.7	34.8	34.9	34.9	34.9
37. $C_2H_4 \rightarrow CH_2C + H_2$	0.0	32.3	34.3	36.2	37.0	37.2	37.2	37.1	36.9	36.7	36.5
38. $CH_2C \rightarrow HCHC$	0.0	0.1	0.1	0.1	0.1	0.2	0.2	0.3	0.3	0.3	0.3
39. $HCHC \rightarrow C_2H_2$	0.0	−4.5	−4.2	−3.7	−3.4	−3.3	−3.2	−3.1	−3.0	−2.9	−2.9
40. $C_2H_6 \rightarrow CH_3CH(s) + H_2$	0.0	32.3	33.5	34.7	34.9	34.7	34.4	34.0	33.6	33.1	32.7
41. $C_2H_4 \rightarrow CH_3CH(s)$	0.0	3.0	2.9	2.7	2.4	2.1	1.9	1.7	1.5	1.3	1.2
42. $CH_3CH(s) \rightarrow C_2H_2 + H_2$	0.0	24.9	27.3	30.0	31.3	32.0	32.4	32.6	32.7	32.8	32.8
43. $C_2H_4 + H \rightarrow C_2H_3 + H_2$	0.0	7.1	7.5	7.7	7.6	7.3	7.0	6.7	6.5	6.2	6.0
44. $C_2H_3 \rightarrow C_2H_2 + H$	0.0	20.9	22.8	25.0	26.1	26.8	27.2	27.5	27.7	27.9	28.0
45. $C_2H_3 + H \rightarrow C_2H_2 + H_2$	0.0	−2.7	−1.7	−0.7	−0.4	−0.4	−0.4	−0.6	−0.7	−0.8	−0.9
46. $C_2H_3 + CH_4 \rightarrow C_2H_4 + CH_3$	0.0	−1.2	−0.8	−0.2	0.1	0.3	0.4	0.4	0.4	0.5	0.5
47. $C_2H_3 + C_2H_6 \rightarrow C_2H_4 + C_2H_5$	0.0	3.2	3.6	4.0	4.3	4.5	4.5	4.6	4.6	4.6	4.7
48. $C_2H_3 + C_2H_5 \rightarrow C_2H_4 + C_2H_4$	0.0	−11.7	−12.4	−13.1	−13.5	−13.6	−13.8	−13.8	−13.9	−13.9	−14.0
49. $C_2H_2 + H \rightarrow C_2H + H_2$	0.0	3.9	3.5	2.8	2.2	1.6	1.2	0.8	0.4	0.1	−0.1
50. $C_2H_6 + CH_3 \rightarrow C_2H_5 + CH_4$	0.0	4.3	4.3	4.3	4.2	4.2	4.2	4.2	4.2	4.2	4.2
51. $C_2H_6 + {}^3CH_2 \rightarrow C_2H_5 + CH_3$	0.0	6.3	6.9	7.6	7.9	8.1	8.2	8.2	8.3	8.3	8.3
52. $C_2H_4 + HCl \rightarrow C_2H_5Cl$	0.0	−31.4	−32.0	−32.3	−32.2	−31.8	−31.5	−31.1	−30.8	−30.5	−30.2
53. $C_2H_2 + HCl \rightarrow C_2H_3Cl$	0.0	−30.7	−32.2	−33.5	−33.8	−33.8	−33.7	−33.5	−33.3	−33.2	−33.0
54. $C_2H_5 + HCl \rightarrow C_2H_5Cl + H$	0.0	−12.4	−12.5	−12.1	−11.5	−11.0	−10.6	−10.2	−9.8	−9.5	−9.3
55. $C_2H_5 + HCl \rightarrow C_2H_6 + Cl$	0.0	−13.1	−13.9	−14.6	−14.8	−14.7	−14.6	−14.4	−14.2	−14.1	−13.9
56. $C_2H_3 + HCl \rightarrow C_2H_3Cl + H$	0.0	−9.8	−9.4	−8.5	−7.7	−7.0	−6.4	−6.0	−5.6	−5.3	−5.0
57. $C_2H_3 + HCl \rightarrow C_2H_4 + Cl$	0.0	−9.9	−10.3	−10.6	−10.5	−10.3	−10.0	−9.8	−9.6	−9.4	−9.3
58. $^3CH_2 + HCl \rightarrow CH_3 + Cl$	0.0	−6.8	−7.0	−7.0	−6.8	−6.6	−6.4	−6.2	−6.0	−5.8	−5.6
59. $^3CH_2 + HCl \rightarrow CH_2Cl + H$	0.0	−4.1	−3.9	−3.2	−2.5	−1.9	−1.4	−1.0	−0.6	−0.3	−0.1
60. $SiCl_3 + SiCl_3 \rightarrow SiCl_2 + SiCl_4$	0.0	−6.2	−6.2	−6.2	−6.2	−6.2	−6.2	−6.2	−6.2	−6.2	−6.2
61. $SiCl_2 + SiCl_3 \rightarrow Si_2Cl_5$	0.0	−35.2	−34.3	−32.9	−31.8	−30.9	−30.2	−29.6	−29.1	−28.7	−28.2
62. $SiCl_2 + SiCl_2 \rightarrow Si_2Cl_4$	0.0	−36.1	−35.1	−33.6	−32.5	−31.7	−31.0	−30.4	−29.8	−29.4	−29.0
63. $SiCl_3 + SiCl_3 \rightarrow Si_2Cl_6$	0.0	−42.2	−41.2	−39.8	−38.8	−37.9	−37.2	−36.6	−36.1	−35.6	−35.2
64. $SiCl_2 + SiCl_4 \rightarrow Si_2Cl_6$	0.0	−36.0	−35.1	−33.7	−32.6	−31.7	−31.0	−30.4	−29.9	−29.4	−29.0
65. $SiCl_3 \rightarrow SiCl_2 + Cl$	0.0	28.8	28.8	28.7	28.5	28.3	28.1	28.0	27.9	27.7	27.6
66. $SiCl_4 \rightarrow SiCl_3 + Cl$	0.0	35.0	35.0	34.8	34.6	34.5	34.3	34.2	34.0	33.9	33.8
67. $SiCl_4 + H_2 \rightarrow SiHCl_3 + HCl$	0.0	9.1	8.1	7.0	6.4	6.1	6.0	5.9	5.8	5.8	5.8
68. $SiCl_3 + H_2 \rightarrow SiHCl_3 + H$	0.0	−5.1	−5.2	−5.0	−4.6	−4.1	−3.7	−3.3	−3.0	−2.6	−2.4
69. $SiCl_3 + H_2 \rightarrow SiHCl_2 + HCl$	0.0	7.7	6.8	5.8	5.3	5.0	4.9	4.8	4.8	4.8	4.8
70. $SiCl_3 + HCl \rightarrow SiCl_4 + H$	0.0	−14.2	−13.4	−12.0	−11.0	−10.2	−9.6	−9.2	−8.8	−8.5	−8.2
71. $SiCl_3 + HCl \rightarrow SiHCl_3 + Cl$	0.0	−8.0	−8.1	−7.9	−7.5	−7.1	−6.7	−6.4	−6.1	−5.9	−5.6
72. $SiCl_2 + H_2 \rightarrow SiH_2Cl_2$	0.0	−30.1	−31.1	−31.8	−31.8	−31.5	−31.1	−30.7	−30.4	−30.0	−29.7
73. $SiCl_2 + H_2 \rightarrow SiHCl + HCl$	0.0	6.0	5.3	4.4	4.0	3.7	3.6	3.6	3.6	3.6	3.6

TABLE 3 (Continued)

reaction	0 K	298.15 K	400 K	600 K	800 K	1000 K	1200 K	1400 K	1600 K	1800 K	2000 K
74. $SiCl_2 + H_2 \rightarrow SiHCl_2 + H$	0.0	−0.4	−0.4	0.0	0.5	1.0	1.4	1.8	2.2	2.5	2.8
75. $SiCl_2 + HCl \rightarrow SiCl_3 + H$	0.0	−8.1	−7.2	−5.8	−4.8	−4.1	−3.5	−3.0	−2.6	−2.3	−2.0
76. $SiCl_2 + HCl \rightarrow SiHCl_2 + Cl$	0.0	−3.2	−3.2	−2.9	−2.4	−2.0	−1.6	−1.3	−1.0	−0.7	−0.5
77. $SiHCl_3 \rightarrow SiCl_2 + HCl$	0.0	36.8	36.9	36.5	35.9	35.3	34.8	34.4	34.0	33.6	33.3
78. $SiHCl_3 \rightarrow SiCl_3 + H$	0.0	28.7	29.7	30.7	31.1	31.3	31.4	31.4	31.4	31.3	31.3
79. $SiHCl_2 \rightarrow SiCl_2 + H$	0.0	23.9	24.8	25.7	26.1	26.2	26.3	26.3	26.2	26.2	26.1
80. $SiHCl_3 \rightarrow SiHCl_2 + Cl$	0.0	33.6	33.7	33.6	33.5	33.4	33.2	33.1	33.0	32.9	32.8
81. $SiH_2Cl_2 \rightarrow SiHCl_2 + H$	0.0	29.7	30.7	31.8	32.2	32.4	32.5	32.5	32.5	32.5	32.5
82. $SiH_2Cl_2 \rightarrow SiH_2Cl + Cl$	0.0	32.0	32.3	32.3	32.3	32.2	32.0	31.9	31.8	31.7	31.6
83. $SiH_2Cl_2 \rightarrow SiHCl + HCl$	0.0	36.1	36.4	36.2	35.7	35.2	34.7	34.3	33.9	33.6	33.3
84. $SiHCl_3 + H_2 \rightarrow SiH_2Cl_2 + HCl$	0.0	6.7	5.8	4.7	4.2	3.9	3.7	3.6	3.6	3.6	3.6
85. $SiHCl_2 + H_2 \rightarrow SiH_2Cl_2 + H$	0.0	−6.1	−6.3	−6.1	−5.7	−5.3	−4.9	−4.5	−4.1	−3.8	−3.6
86. $SiHCl_2 + HCl \rightarrow SiHCl_3 + H$	0.0	−12.9	−12.1	−10.8	−9.9	−9.1	−8.6	−8.1	−7.7	−7.4	−7.2
87. $SiHCl_2 + HCl \rightarrow SiH_2Cl_2 + Cl$	0.0	−9.0	−9.1	−9.0	−8.6	−8.2	−7.9	−7.6	−7.3	−7.0	−6.8
88. $SiHCl + H_2 \rightarrow SiH_3Cl$	0.0	−31.4	−32.5	−33.3	−33.3	−33.1	−32.8	−32.4	−32.1	−31.7	−31.4
89. $SiHCl + HCl \rightarrow SiHCl_2 + H$	0.0	−6.4	−5.7	−4.4	−3.5	−2.8	−2.2	−1.8	−1.4	−1.1	−0.8
90. $SiHCl + HCl \rightarrow SiH_2Cl + Cl$	0.0	−4.1	−4.2	−3.9	−3.5	−3.1	−2.7	−2.4	−2.1	−1.9	−1.6
91. $SiCl_3 + CH_4 \rightarrow CH_3SiCl_3 + H$	0.0	−10.3	−8.9	−6.6	−5.0	−3.9	−3.0	−2.3	−1.7	−1.2	−0.8
92. $SiCl_3 + CH_4 \rightarrow SiHCl_3 + CH_3$	0.0	0.8	1.5	2.5	3.1	3.5	3.7	3.8	4.0	4.0	4.1
93. $SiCl_3 + CH_3 \rightarrow SiCl_2 + CH_3Cl$	0.0	0.2	−1.0	−2.3	−3.0	−3.3	−3.4	−3.5	−3.6	−3.6	−3.6
94. $SiCl_3 + CH_3 \rightarrow SiHCl_3 + {}^3CH_2$	0.0	−1.2	−1.1	−0.9	−0.6	−0.4	−0.3	−0.2	−0.1	−0.1	0.0
95. $SiCl_2 + CH_4 \rightarrow CH_3SiHCl_2$	0.0	−33.2	−32.7	−31.4	−30.2	−29.2	−28.4	−27.7	−27.1	−26.6	−26.1
96. $SiCl_2 + CH_4 \rightarrow SiHCl_2 + CH_3$	0.0	5.5	6.3	7.5	8.1	8.5	8.8	9.0	9.1	9.2	9.2
97. $CH_2SiCl_2 + H_2 \rightarrow CH_3SiHCl_2$	0.0	−27.6	−28.8	−29.9	−30.2	−30.1	−29.9	−29.6	−29.3	−29.0	−28.8
98. $CH_3SiHCl_2 \rightarrow CH_2SiHCl + HCl$	0.0	34.3	34.7	34.8	34.6	34.2	33.9	33.5	33.2	32.9	32.6
99. $CH_3SiCl_2 + H_2 \rightarrow CH_3SiHCl_2 + H$	0.0	−5.0	−5.1	−4.9	−4.5	−4.0	−3.6	−3.2	−2.9	−2.6	−2.3
100. $CH_2SiCl_3 + H_2 \rightarrow CH_3SiCl_3 + H$	0.0	−10.3	−10.9	−11.4	−11.3	−11.2	−10.9	−10.6	−10.4	−10.1	−9.9
101. $CH_3 + CH_3SiCl_3 \rightarrow CH_4 + CH_2SiCl_3$	0.0	4.4	4.2	3.9	3.7	3.6	3.5	3.5	3.5	3.4	3.4
102. $CH_3 + CH_3SiCl_3 \rightarrow CH_3Cl + CH_3SiCl_2$	0.0	5.9	4.7	3.5	2.9	2.6	2.5	2.4	2.3	2.3	2.2
103. $SiCl_3 + CH_3SiCl_3 \rightarrow SiHCl_3 + CH_2SiCl_3$	0.0	5.1	5.6	6.4	6.8	7.0	7.2	7.3	7.4	7.5	7.5
104. $SiCl_3 + CH_3SiCl_3 \rightarrow SiCl_4 + CH_3SiCl_2$	0.0	−0.4	−0.4	−0.4	−0.3	−0.3	−0.3	−0.3	−0.3	−0.3	−0.3
105. $H + CH_3SiCl_3 \rightarrow HCl + CH_3SiCl_2$	0.0	13.8	13.0	11.7	10.7	9.9	9.3	8.9	8.5	8.2	7.9
106. $Cl + CH_3SiCl_3 \rightarrow HCl + CH_2SiCl_3$	0.0	13.1	13.7	14.2	14.2	14.1	13.9	13.7	13.5	13.3	13.2
107. $CH_2SiCl_3 \rightarrow {}^3CH_2 + SiCl_3$	0.0	33.5	33.3	32.6	31.8	31.1	30.5	29.9	29.4	29.0	28.6
108. $CH_2SiCl_3 \rightarrow CH_2SiCl_2 + Cl$	0.0	23.2	22.9	22.4	22.1	21.9	21.7	21.5	21.4	21.3	21.2
109. $CH_3SiCl_2 \rightarrow CH_3 + SiCl_2$	0.0	34.1	34.3	34.0	33.4	32.7	32.1	31.6	31.1	30.7	30.3
110. $CH_3SiCl_2 \rightarrow H + CH_2SiCl_2$	0.0	22.5	23.7	25.0	25.7	26.1	26.3	26.4	26.4	26.5	26.5
111. $CH_3SiCl_3 \rightarrow CH_3SiCl_2Cl$	0.0	8.1	8.2	8.4	8.4	8.5	8.5	8.5	8.5	8.5	8.5
112. $CH_3SiCl_2Cl \rightarrow CH_3SiCl + Cl_2$	0.0	33.2	32.7	31.9	31.2	30.6	30.1	29.7	29.4	29.0	28.7
113. $CH_3SiCl + H_2 \rightarrow CH_3SiH_2Cl$	0.0	−31.2	−32.4	−33.2	−33.3	−33.0	−32.7	−32.3	−32.0	−31.6	−31.3
114. $CH_3SiCl + HCl \rightarrow CH_3SiHCl_2$	0.0	−37.2	−37.4	−37.2	−36.7	−36.2	−35.7	−35.3	−34.9	−34.5	−34.2

in the gas chromatography experiments done by Mousavipour et al.[8] It is natural to include reactions involving the above species in the reaction mechanism. Another strategy is to review the gas-phase reaction mechanism proposed by others, such as Allendorf et al.,[1] Osterheld et al.,[23] Zhang et al.,[21,22] and Sotirchos et al.,[12,13] to select reasonable reactions that might significantly affect the gas-phase composition. Some reactions proposed by others may be excluded. For example, the gas-phase polymerization reactions of $SiCl_2$ and CH_3SiCl proposed by Zhang and Huttinger[21,22] may be excluded, because such reactions tend not to be important at the high temperatures of interest here, because they are entropically disfavored. The energy decrease due to the formation of one extra Si−Si single bond during the growth of a Si chain may not compensate the Gibbs free energy increase contributed by the loss of the translational entropy of one monomer. The concentration of MTS decreases quickly in the early stage of high-temperature CVD.[12] The major decomposition pathway of MTS is to break the Si−C bond to form CH_3 and $SiCl_3$ radicals at typical CVD temperatures,[7,23] even though a typical Si−C bond is about 23 kcal/mol stronger than a typical Si−Si bond. A third strategy is to look up the reaction rate constants obtained experimentally and/or theoretically[48] as a guide in choosing significant reactions. Reactions with low reported reaction rate constants and reactants with low concentration might be removed from the reaction list for the proposed mechanism. However, this must be done with a great deal of caution because the reaction rate constants obtained from various experiments and theoretical calculations do not often agree well with each other and it is often difficult to predict the concentration of reactants. Consequently, no reactions are initially eliminated in the present study.

Enthalpy, entropy and Gibbs free energy changes for the decomposition reactions of MTS and the consecutive reactions in the gas phase at various temperatures from 0 to 2000 K are reported in Tables 2−4 respectively. Table 2 shows that the enthalpy changes of all 114 reactions are not sensitive to temperature change. For example, the reaction enthalpy of $CH_3SiCl_3 \rightarrow CH_3 + SiCl_3$ is 91.6, 91.9, 88.3 kcal/mol at 0, 1000, 2000 K, respectively. Table 3 shows that the magnititudes of reaction entropies are usually less than 10 cal/(mol K) in the range 0−2000 K, if the numbers of reactant and product particles are equal. However, reaction entropies increase by ca. 20−40 cal/(mol K) if products outnumber reactants by 1, or vice versa. This is mainly due to the contribution of the translational entropy of the extra particle. Reaction entropies may significantly affect Gibbs free energy changes at high tempertures. Table 4 shows that free energy changes of reactions with a greater number of particles on the product side decrease dramatically as the temperature increases, and vice versa. For example, $CH_3SiCl_3 \rightarrow CH_3 + SiCl_3$ has reaction Gibbs free energies of 91.6, 53.3, 16.0 kcal/mol at 0, 1000, and 2000 K respectively. The 114

TABLE 4: Gibbs Free Energy Changes (kcal/mol) of the Decomposition Reactions of CH_3SiCl_3 and Consecutive Reactions in the Gas Phase at Various Temperatures

reaction	0 K	298.15 K	400 K	600 K	800 K	1000 K	1200 K	1400 K	1600 K	1800 K	2000 K
1. $CH_3SiCl_3 \rightarrow CH_3 + SiCl_3$	91.6	81.1	77.0	69.0	61.1	53.3	45.7	38.1	30.7	23.3	16.0
2. $CH_3SiCl_3 \rightarrow H + CH_2SiCl_3$	101.1	92.7	89.2	81.9	74.4	66.8	59.1	51.4	43.6	35.9	28.1
3. $CH_3SiCl_3 \rightarrow Cl + CH_3SiCl_2$	108.4	98.8	95.3	88.4	81.5	74.7	67.9	61.1	54.3	47.6	40.9
4. $CH_3SiCl_3 \rightarrow CH_2SiCl_2 + HCl$	78.8	69.0	65.3	58.0	50.7	43.4	36.3	29.2	22.2	15.2	8.3
5. $CH_3SiCl_3 \rightarrow CH_3Cl + SiCl_2$	72.6	61.1	57.1	49.4	42.1	34.9	27.9	21.1	14.3	7.7	1.2
6. $CH_3SiCl_3 \rightarrow {}^1CH_2 + SiHCl_3$	118.2	108.4	104.6	97.1	89.7	82.4	75.1	68.0	60.9	53.9	46.9
7. $CH_3SiCl_3 \rightarrow {}^1CHSiCl_3 + H_2$	119.7	112.0	108.7	101.9	95.0	88.0	81.1	74.1	67.2	60.4	53.6
8. $CH_3SiCl_3 \rightarrow CH_3SiCl + Cl_2$	128.3	116.7	112.6	104.4	96.4	88.6	80.8	73.1	65.5	58.0	50.5
9. $H_2 \rightarrow H + H$	102.8	96.6	94.2	89.1	83.9	78.5	73.1	67.5	61.8	56.1	50.4
10. $HCl \rightarrow H + Cl$	101.2	95.9	93.8	89.3	84.7	79.9	75.0	70.0	65.0	59.9	54.8
11. $Cl_2 \rightarrow Cl + Cl$	53.8	47.9	45.5	40.9	36.1	31.3	26.4	21.5	16.6	11.6	6.6
12. $Cl + H_2 \rightarrow HCl + H$	1.5	0.7	0.4	−0.2	−0.8	−1.4	−1.9	−2.6	−3.2	−3.8	−4.5
13. $Cl + HCl \rightarrow Cl_2 + H$	47.4	48.1	48.2	48.5	48.6	48.6	48.6	48.5	48.4	48.3	48.2
14. $CH_3 + H_2 \rightarrow CH_4 + H$	0.5	1.5	2.2	3.6	5.1	6.6	8.1	9.6	11.0	12.3	13.7
15. $CH_3 + H \rightarrow {}^3CH_2 + H_2$	5.0	4.3	3.9	3.1	2.3	1.5	0.8	0.2	−0.4	−1.0	−1.5
16. $CH_3 + H \rightarrow CH_4$	−102.3	−95.1	−92.0	−85.5	−78.8	−71.9	−64.9	−57.9	−50.8	−43.8	−36.7
17. $CH_3 + CH_3 \rightarrow C_2H_6$	−86.6	−77.2	−73.2	−64.9	−56.5	−48.0	−39.7	−31.4	−23.1	−15.0	−6.9
18. $CH_3 + CH_3 \rightarrow C_2H_5 + H$	12.4	13.4	13.9	14.9	15.7	16.4	17.0	17.4	17.7	18.0	18.1
19. $CH_3 + CH_3 \rightarrow {}^3CH_2 + CH_4$	5.5	5.8	6.1	6.7	7.4	8.2	8.9	9.7	10.6	11.4	12.2
20. $CH_3 \rightarrow {}^3CH_2 + H$	107.8	100.9	98.1	92.2	86.2	80.1	73.9	67.6	61.4	55.1	48.9
21. $CH_3 + HCl \rightarrow CH_3Cl + H$	20.5	22.2	23.0	24.7	26.3	27.8	29.2	30.5	31.8	33.0	34.2
22. $CH_3 + HCl \rightarrow CH_4 + Cl$	−1.0	0.9	1.8	3.8	5.9	8.0	10.1	12.1	14.2	16.2	18.1
23. $CH_3Cl + H_2 \rightarrow CH_4 + HCl$	−20.0	−20.7	−20.9	−21.1	−21.2	−21.2	−21.1	−21.0	−20.8	−20.7	−20.5
24. $CH_2Cl + HCl \rightarrow CH_2Cl_2 + H$	24.0	27.3	28.6	31.1	33.5	35.7	37.9	40.0	42.0	43.9	45.8
25. ${}^3CH_2 + CH_3 \rightarrow C_2H_5$	−95.4	−87.5	−84.2	−77.3	−70.5	−63.6	−56.9	−50.2	−43.7	−37.2	−30.8
26. ${}^3CH_2 + CH_3 \rightarrow C_2H_4 + H$	−60.3	−57.2	−55.8	−53.0	−50.2	−47.5	−44.9	−42.5	−40.1	−37.8	−35.6
27. ${}^3CH_2 + {}^3CH_2 \rightarrow C_2H_2 + H + H$	−25.4	−27.7	−28.8	−31.5	−34.6	−37.9	−41.5	−45.2	−49.1	−53.1	−57.2
28. ${}^3CH_2 + {}^3CH_2 \rightarrow C_2H_2 + H_2$	−128.1	−124.3	−123.0	−120.6	−118.5	−116.4	−114.5	−112.7	−110.9	−109.2	−107.5
29. $C_2H_6 \rightarrow C_2H_5 + H$	98.9	90.6	87.1	79.8	72.2	64.4	56.6	48.8	40.9	33.0	25.1
30. $C_2H_6 \rightarrow C_2H_4 + H_2$	31.3	24.4	21.3	15.0	8.6	2.1	−4.5	−10.9	−17.4	−23.8	−30.1
31. $C_2H_6 \rightarrow C_2H_6(e)$	2.5	2.2	2.2	2.4	2.7	3.2	3.7	4.2	4.9	5.5	6.3
32. $C_2H_6(e) \rightarrow C_2H_4 + H_2$	28.8	22.2	19.1	12.6	5.8	−1.1	−8.1	−15.2	−22.2	−29.3	−36.4
33. $C_2H_6 + H \rightarrow C_2H_5 + H_2$	−3.8	−6.0	−7.1	−9.4	−11.7	−14.1	−16.4	−18.7	−21.0	−23.2	−25.3
34. $C_2H_5 \rightarrow C_2H_4 + H$	35.1	30.3	28.4	24.4	20.3	16.2	12.0	7.8	3.6	−0.6	−4.8
35. $C_2H_5 + H \rightarrow C_2H_4 + H_2$	−67.7	−66.3	−65.8	−64.7	−63.6	−62.4	−61.1	−59.7	−58.2	−56.7	−55.2
36. $C_2H_4 \rightarrow C_2H_3 + H$	109.9	102.3	99.1	92.5	85.8	78.9	72.0	65.0	58.1	51.1	44.1
37. $C_2H_4 \rightarrow CH_2C + H_2$	82.1	74.8	71.4	64.3	57.0	49.5	42.1	34.7	27.3	19.9	12.6
38. $CH_2C \rightarrow HCHC$	1.3	1.2	1.2	1.1	1.1	1.1	1.1	1.0	1.0	0.9	0.8
39. $HCHC \rightarrow C_2H_2$	−43.5	−42.1	−41.7	−40.9	−40.2	−39.5	−38.9	−38.3	−37.7	−37.1	−36.5
40. $C_2H_6 \rightarrow CH_3CH(s) + H_2$	104.4	96.6	93.3	86.4	79.5	72.5	65.6	58.7	52.0	45.3	38.7
41. $C_2H_4 \rightarrow CH_3CH(s)$	73.2	72.3	71.9	71.4	70.9	70.4	70.0	69.7	69.3	69.1	68.8
42. $CH_3CH(s) \rightarrow C_2H_2 + H_2$	−33.2	−38.4	−41.1	−46.9	−53.0	−59.3	−65.8	−72.3	−78.8	−85.3	−91.9
43. $C_2H_4 + H \rightarrow C_2H_3 + H_2$	7.2	5.7	4.9	3.4	1.9	0.4	−1.1	−2.4	−3.8	−5.0	−6.2
44. $C_2H_3 \rightarrow C_2H_2 + H$	32.8	28.2	25.9	21.1	16.0	10.7	5.3	−0.2	−5.7	−11.3	−16.8
45. $C_2H_3 + H \rightarrow C_2H_2 + H_2$	−69.9	−68.4	−68.2	−68.0	−67.9	−67.8	−67.7	−67.6	−67.5	−67.4	−67.2
46. $C_2H_3 + CH_4 \rightarrow C_2H_4 + CH_3$	−7.7	−7.2	−7.1	−7.0	−7.0	−7.0	−7.1	−7.2	−7.2	−7.3	−7.4
47. $C_2H_3 + C_2H_6 \rightarrow C_2H_4 + C_2H_5$	−11.0	−11.6	−12.0	−12.8	−13.6	−14.5	−15.4	−16.3	−17.2	−18.1	−19.1
48. $C_2H_3 + C_2H_5 \rightarrow C_2H_4 + C_2H_4$	−74.9	−71.9	−70.7	−68.1	−65.5	−62.8	−60.0	−57.3	−54.5	−51.7	−48.9
49. $C_2H_2 + H \rightarrow C_2H + H_2$	31.8	30.9	30.5	29.9	29.4	29.0	28.7	28.5	28.4	28.4	28.4
50. $C_2H_6 + CH_3 \rightarrow C_2H_5 + CH_4$	−3.3	−4.5	−4.9	−5.8	−6.6	−7.5	−8.3	−9.1	−10.0	−10.8	−11.6
51. $C_2H_6 + {}^3CH_2 \rightarrow C_2H_5 + CH_3$	−8.8	−10.3	−11.0	−12.4	−14.0	−15.6	−17.2	−18.9	−20.5	−22.2	−23.8
52. $C_2H_4 + HCl \rightarrow C_2H_5Cl$	−16.3	−8.5	−5.2	1.2	7.7	14.1	20.4	26.7	32.9	39.0	45.1
53. $C_2H_2 + HCl \rightarrow C_2H_3Cl$	−25.1	−17.8	−14.6	−8.0	−1.3	5.5	12.2	18.9	25.6	32.3	38.9
54. $C_2H_5 + HCl \rightarrow C_2H_5Cl + H$	18.7	21.9	23.2	25.6	28.0	30.2	32.4	34.5	36.5	38.4	40.3
55. $C_2H_5 + HCl \rightarrow C_2H_6 + Cl$	2.3	5.3	6.7	9.6	12.5	15.5	18.4	21.3	24.1	27.0	29.8
56. $C_2H_3 + HCl \rightarrow C_2H_3Cl + H$	7.7	10.4	11.3	13.1	14.7	16.2	17.5	18.8	19.9	21.0	22.1
57. $C_2H_3 + HCl \rightarrow C_2H_4 + Cl$	−8.7	−6.3	−5.3	−3.2	−1.1	1.0	3.0	5.0	6.9	8.8	10.7
58. ${}^3CH_2 + HCl \rightarrow CH_3 + Cl$	−6.6	−5.0	−4.3	−2.9	−1.5	−0.2	1.1	2.4	3.6	4.8	5.9
59. ${}^3CH_2 + HCl \rightarrow CH_2Cl + H$	10.6	11.5	11.9	12.6	13.2	13.6	14.0	14.2	14.4	14.4	14.5
60. $SiCl_3 + SiCl_3 \rightarrow SiCl_2 + SiCl_4$	−43.8	−41.9	−41.3	−40.1	−38.8	−37.6	−36.4	−35.1	−33.9	−32.7	−31.4
61. $SiCl_2 + SiCl_3 \rightarrow Si_2Cl_5$	−34.2	−23.5	−20.0	−13.3	−6.8	−0.5	5.6	11.6	17.5	23.2	28.9
62. $SiCl_2 + SiCl_2 \rightarrow Si_2Cl_4$	−12.9	−1.9	1.7	8.6	15.2	21.6	27.9	34.0	40.0	46.0	51.8
63. $SiCl_3 + SiCl_3 \rightarrow Si_2Cl_6$	−76.4	−63.6	−59.4	−51.3	−43.4	−35.8	−28.3	−20.9	−13.6	−6.4	0.6
64. $SiCl_2 + SiCl_4 \rightarrow Si_2Cl_6$	−32.7	−21.7	−18.1	−11.2	−4.6	1.8	8.1	14.2	20.3	26.2	32.1
65. $SiCl_3 \rightarrow SiCl_2 + Cl$	61.7	53.8	50.8	45.1	39.4	33.7	28.1	22.4	16.9	11.3	5.8
66. $SiCl_4 \rightarrow SiCl_3 + Cl$	105.5	95.7	92.1	85.1	78.2	71.3	64.4	57.6	50.8	44.0	37.2
67. $SiCl_4 + H_2 \rightarrow SiHCl_3 + HCl$	17.0	13.5	12.7	11.2	9.8	8.6	7.4	6.2	5.0	3.8	2.7
68. $SiCl_3 + H_2 \rightarrow SiHCl_3 + H$	12.8	13.8	14.3	15.3	16.3	17.2	17.9	18.6	19.3	19.8	20.3
69. $SiCl_3 + H_2 \rightarrow SiHCl_2 + HCl$	18.2	15.2	14.4	13.2	12.1	11.1	10.1	9.1	8.1	7.2	6.2
70. $SiCl_3 + HCl \rightarrow SiCl_4 + H$	−4.3	0.2	1.7	4.2	6.5	8.6	10.6	12.5	14.3	16.0	17.7
71. $SiCl_3 + HCl \rightarrow SiHCl_3 + Cl$	11.3	13.1	13.9	15.5	17.1	18.5	19.9	21.2	22.5	23.7	24.8
72. $SiCl_2 + H_2 \rightarrow SiH_2Cl_2$	−31.9	−24.8	−21.7	−15.4	−9.0	−2.7	3.6	9.8	15.9	21.9	27.9
73. $SiCl_2 + H_2 \rightarrow SiHCl + HCl$	29.7	27.5	26.9	26.0	25.1	24.4	23.6	22.9	22.2	21.5	20.8

TABLE 4 (Continued)

reaction	0 K	298.15 K	400 K	600 K	800 K	1000 K	1200 K	1400 K	1600 K	1800 K	2000 K
74. $SiCl_2 + H_2 \rightarrow SiHCl_2 + H$	57.7	57.4	57.4	57.4	57.4	57.2	57.0	56.7	56.3	55.8	55.3
75. $SiCl_2 + HCl \rightarrow SiCl_3 + H$	39.5	42.2	42.9	44.2	45.3	46.2	46.9	47.6	48.2	48.6	49.1
76. $SiCl_2 + HCl \rightarrow SiHCl_2 + Cl$	56.2	56.7	57.0	57.6	58.2	58.6	59.0	59.2	59.5	59.6	59.8
77. $SiHCl_3 \rightarrow SiCl_2 + HCl$	50.4	40.7	36.9	29.6	22.3	15.2	8.2	1.2	−5.6	−12.3	−19.0
78. $SiHCl_3 \rightarrow SiCl_3 + H$	90.0	82.8	79.8	73.8	67.6	61.4	55.1	48.8	42.6	36.3	30.0
79. $SiHCl_2 \rightarrow SiCl_2 + H$	45.0	39.3	36.8	31.7	26.5	21.3	16.0	10.8	5.5	0.3	−4.9
80. $SiHCl_3 \rightarrow SiHCl_2 + Cl$	106.7	97.3	93.9	87.2	80.5	73.8	67.1	60.5	53.9	47.3	40.7
81. $SiH_2Cl_2 \rightarrow SiHCl_2 + H$	89.6	82.1	79.1	72.8	66.4	59.9	53.4	46.9	40.4	33.9	27.4
82. $SiH_2Cl_2 \rightarrow SiH_2Cl + Cl$	106.3	97.7	94.4	87.9	81.5	75.0	68.6	62.2	55.8	49.5	43.1
83. $SiH_2Cl_2 \rightarrow SiHCl + HCl$	61.6	52.3	48.6	41.3	34.1	27.0	20.0	13.1	6.3	−0.4	−7.1
84. $SiHCl_3 + H_2 \rightarrow SiH_2Cl_2 + HCl$	18.6	15.9	15.2	14.2	13.3	12.5	11.8	11.0	10.3	9.6	8.8
85. $SiHCl_2 + H_2 \rightarrow SiH_2Cl_2 + H$	13.1	14.5	15.1	16.3	17.5	18.6	19.6	20.6	21.4	22.2	23.0
86. $SiHCl_2 + HCl \rightarrow SiHCl_3 + H$	−5.4	−1.4	−0.1	2.2	4.2	6.1	7.9	9.5	11.1	12.6	14.1
87. $SiHCl_2 + HCl \rightarrow SiH_2Cl_2 + Cl$	11.6	13.8	14.7	16.5	18.3	20.0	21.6	23.1	24.6	26.0	27.4
88. $SiHCl + H_2 \rightarrow SiH_3Cl$	−43.4	−35.9	−32.6	−26.0	−19.4	−12.7	−6.1	0.4	6.9	13.2	19.6
89. $SiHCl + HCl \rightarrow SiHCl_2 + H$	28.0	29.9	30.5	31.5	32.3	32.9	33.4	33.8	34.1	34.4	34.5
90. $SiHCl + HCl \rightarrow SiH_2Cl + Cl$	44.6	45.4	45.8	46.6	47.3	48.0	48.6	49.1	49.5	49.9	50.3
91. $SiCl_3 + CH_4 \rightarrow CH_3SiCl_3 + H$	10.6	14.0	15.0	16.5	17.7	18.6	19.3	19.8	20.2	20.5	20.7
92. $SiCl_3 + CH_4 \rightarrow SiHCl_3 + CH_3$	12.3	12.3	12.1	11.7	11.2	10.5	9.8	9.1	8.3	7.5	6.7
93. $SiCl_3 + CH_3 \rightarrow SiCl_2 + CH_3Cl$	−19.0	−20.0	−19.9	−19.6	−19.0	−18.4	−17.7	−17.0	−16.3	−15.6	−14.9
94. $SiCl_3 + CH_3 \rightarrow SiHCl_3 + {}^3CH_2$	17.8	18.1	18.2	18.4	18.6	18.7	18.8	18.8	18.8	18.9	18.9
95. $SiCl_2 + CH_4 \rightarrow CH_3SiHCl_2$	−33.0	−24.1	−20.8	−14.3	−8.2	−2.2	3.5	9.1	14.6	20.0	25.2
96. $SiCl_2 + CH_4 \rightarrow SiHCl_2 + CH_3$	57.2	55.8	55.2	53.8	52.3	50.6	48.9	47.1	45.3	43.5	41.6
97. $CH_2SiCl_2 + H_2 \rightarrow CH_3SiHCl_2$	−59.2	−52.7	−49.9	−44.0	−37.9	−31.9	−25.9	−20.0	−14.1	−8.2	−2.4
98. $CH_3SiHCl_2 \rightarrow CH_2SiHCl + HCl$	74.2	65.1	61.6	54.6	47.7	40.8	34.0	27.2	20.6	13.9	7.4
99. $CH_3SiCl_2 + H_2 \rightarrow CH_3SiHCl_2 + H$	12.4	13.4	13.9	14.9	15.9	16.7	17.5	18.2	18.8	19.3	19.8
100. $CH_2SiCl_3 + H_2 \rightarrow CH_3SiCl_3 + H$	1.7	3.9	5.0	7.2	9.5	11.8	14.0	16.1	18.2	20.3	22.3
101. $CH_3 + CH_3SiCl_3 \rightarrow CH_4 + CH_2SiCl_3$	−1.2	−2.4	−2.8	−3.6	−4.4	−5.1	−5.8	−6.5	−7.2	−7.9	−8.6
102. $CH_3 + CH_3SiCl_3 \rightarrow CH_3Cl + CH_3SiCl_2$	27.7	25.1	24.6	23.8	23.1	22.6	22.1	21.6	21.1	20.7	20.2
103. $SiCl_3 + CH_3SiCl_3 \rightarrow SiHCl_3 + CH_2SiCl_3$	11.1	9.9	9.3	8.1	6.8	5.4	4.0	2.5	1.1	−0.4	−1.9
104. $SiCl_3 + CH_3SiCl_3 \rightarrow SiCl_4 + CH_3SiCl_2$	3.0	3.1	3.2	3.3	3.3	3.4	3.5	3.5	3.6	3.6	3.7
105. $H + CH_3SiCl_3 \rightarrow HCl + CH_3SiCl_2$	7.2	2.9	1.5	−0.9	−3.2	−5.2	−7.1	−9.0	−10.7	−12.4	−14.0
106. $Cl + CH_3SiCl_3 \rightarrow HCl + CH_2SiCl_3$	−0.1	−3.2	−4.6	−7.4	−10.3	−13.1	−15.9	−18.7	−21.4	−24.1	−26.7
107. $CH_2SiCl_3 \rightarrow {}^3CH_2 + SiCl_3$	98.3	89.3	85.9	79.3	72.9	66.6	60.4	54.4	48.4	42.6	36.8
108. $CH_2SiCl_3 \rightarrow CH_2SiCl_2 + Cl$	79.0	72.3	69.9	65.4	60.9	56.5	52.2	47.8	43.6	39.3	35.0
109. $CH_3SiCl_2 \rightarrow CH_3 + SiCl_2$	44.9	36.0	32.5	25.7	18.9	12.3	5.8	−0.5	−6.8	−13.0	−19.1
110. $CH_3SiCl_2 \rightarrow H + CH_2SiCl_2$	71.6	66.1	63.8	58.9	53.8	48.6	43.4	38.1	32.8	27.6	22.3
111. $CH_3SiCl_3 \rightarrow CH_3SiCl_2Cl$	111.1	109.1	108.3	106.6	105.0	103.3	101.6	99.9	98.2	96.5	94.8
112. $CH_3SiCl_2Cl \rightarrow CH_3SiCl + Cl_2$	17.2	7.6	4.2	−2.2	−8.5	−14.7	−20.8	−26.8	−32.7	−38.5	−44.3
113. $CH_3SiCl + H_2 \rightarrow CH_3SiH_2Cl$	−42.5	−35.1	−31.9	−25.3	−18.6	−12.0	−5.4	1.1	7.5	13.9	20.2
114. $CH_3SiCl + HCl \rightarrow CH_3SiHCl_2$	−62.8	−53.0	−49.2	−41.8	−34.4	−27.1	−19.9	−12.8	−5.8	1.2	8.0

reactions in Tables 2−4 are reactions that may affect the concentration of the various species in the gas phase. Further screening of these reactions will require kinetic simulations to provide accurate rate constants. This data and the corresponding analysis will be provided in subsequent reports.

To evaluate the accuracy of the predictions of thermodynamic properties, experimental reaction enthalpies vs temperature for reactions that only involve CH_4, C_2H_2, C_2H_4, C_2H_6, H, H_2, Cl, Cl_2, and HCl are compared with the experimental heats of formation as a function of temperature[40] in Figure 4. Enthalphy changes of other reactions, such as dehydrogenation reactions, can be derived from the six independent reactions. The four reactions in Figure 4 that do not involve Cl all display excellent agreement between calculations and experiments throughout the temperature range. The discrepancies increase monotonically with temperature. The largest discrepancy between experimental and theoretical reaction enthalpies is found for $Cl_2 \rightarrow 2Cl$, ranging from 3.4 kcal/mol at 298.15 K to 4.1 kcal/mol at 1400 K, increasing monotonically with temperature. This large discrepancy is not surprising, because predicting accurate atomization energies for halogen molecules are known to be difficult. For example, CCSD(T) calculations with the aug-cc-pVDZ or aug-cc-pVTZ basis set produce errors of 9.5 and 2.6 kcal/mol, respectively, for the atomization energy of F_2.[49] The error can be reduced to 1.3 or 0.9 kcal/mol if the larger aug-cc-pVQZ or aug-cc-pV5Z basis sets are used.[49] However, these latter two basis sets are impractical for the large number of calculations that are of interest here.

To evaluate the accuracy of the predicted thermochemical properties of the various radicals investigated, the bond enthalpies predicted in this work are compared in Table 5 with the experimental ones[50] that were obtained at 298 K. The bond enthalpy of a bond homolysis reaction $AB \rightarrow A + B$, $DH(AB)$, is defined as the reaction enthalpy:

$$DH(AB) = \Delta_f H(A) + \Delta_f H(B) - \Delta_f H(AB) \qquad (2)$$

where $\Delta_f H$ stands for the standard enthalpy of formation. Table 5 shows that the largest discrepancy is only 1.3 kcal/mol for $CH_3 + CH_3 \rightarrow C_2H_6$ and $^3CH_2 + H \rightarrow CH_3$ among all of the 9 compared bond fission reactions.

IV. Conclusions

The thermodynamic properties of the unimolecular decomposition reactions of methyltrichlorosilane and other reactions related to the mechanism of the CVD process were studied. Energies and structures of various gas-phase species produced in the gas phase have been presented and discussed. The predicted isobaric heat capacity and entropy values of various gas-phase species agree well with experimental data. Reaction

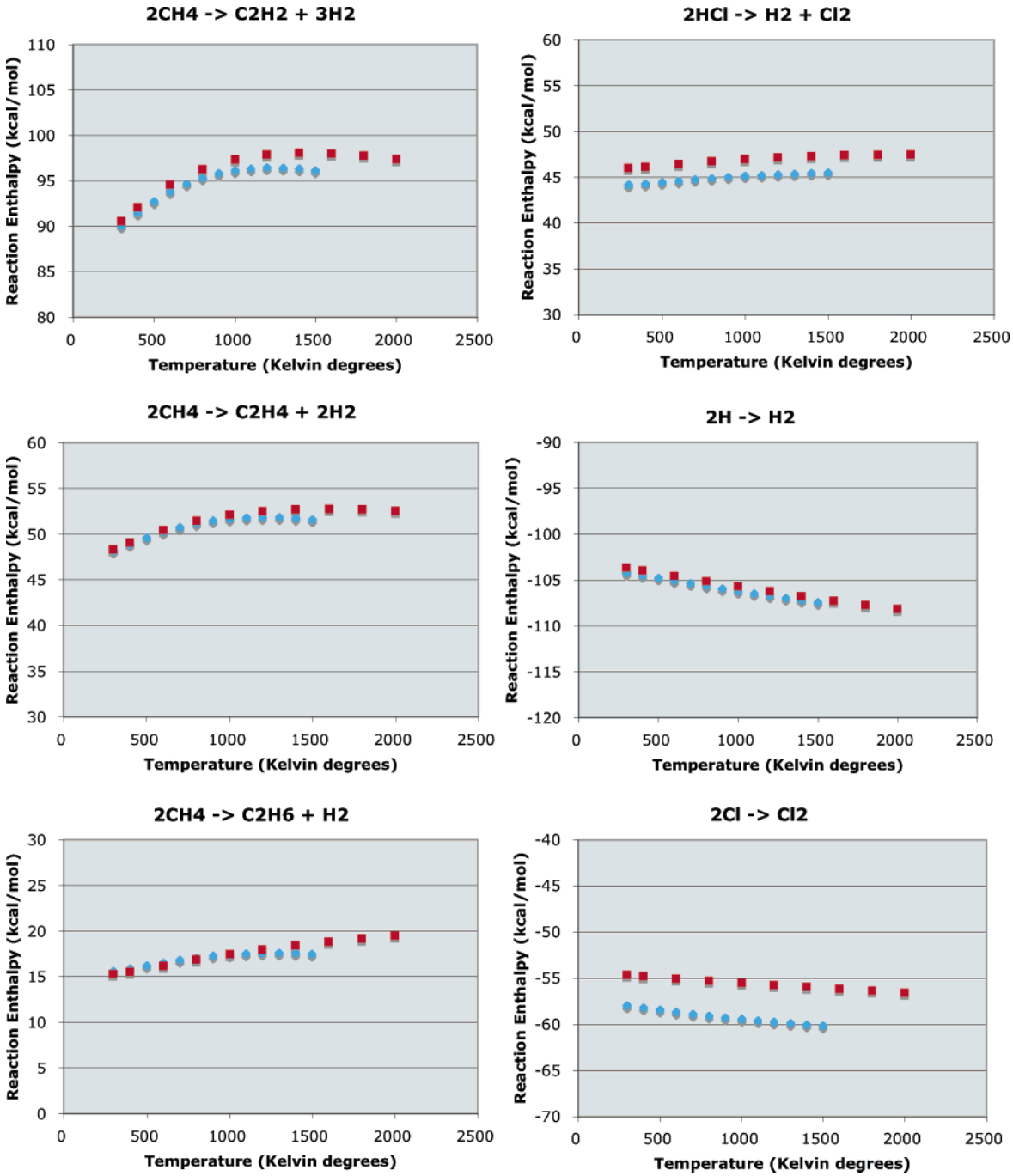

Figure 4. Comparison between predicted (red squares) and experimental (blue rhombus) reaction enthalpies.

TABLE 5: Predicted Bond Enthalpies (kcal/mol) of A + B → AB Type Reactions Compared with Experimental Data at 298 K

A	B	this work	experimental data[50]
H	H	103.6	104.206 ± 0.003
H	Cl	102.1	103.15 ± 0.03
H	CH_3	103.9	104.99 ± 0.03
H	$^3CH_2$	109.1	110.4 ± 0.2
H	CH_2CH_3	100.7	101.1 ± 0.4
H	-CH═CH_2	111.4	110.7 ± 0.6
H	CH_2═CH_2	36.0	35.7 ± 0.7
H	CH═CH	34.4	35.4 ± 0.7
CH_3	CH_3	88.8	90.1 ± 0.1

enthalpies, entropies and Gibbs free energies were also predicted and compare satisfactorily with available experimental values. The details of the transition state structures and the associated barrier heights will be illustrated in a subsequent work.

Acknowledgment. This project is supported by the U.S. Department of Energy, Grant No. DE-FC07-05ID14661. Computer time was provided by the Scalable Computing Laboratory, Iowa State University. We are grateful to Drs. Mike Schmidt and Hui Li for valuable discussions.

Supporting Information Available: Tables of predicted energies, zero point energies, Cartesian coordinates, vibrational frequencies, and values of isobaric heat capacity at atmospheric pressure of all of the species studied in this work, and values of isobaric heat capacity at atmospheric pressure. This material is available free of charge via the Internet at http://pubs.acs.org.

References and Notes

(1) Allendorf, M. D.; Kee, R. J. *J. Electrochem. Soc.* **1991**, *138*, 841.
(2) Sone, H.; Kaneko, T.; Miyakawa, N. *J. Cryst. Growth* **2000**, *219*, 245.

(3) Vorob'ev, A. N.; Karpov, S. Y.; Zhmakin, A. I.; Lovtsus, A. A.; Makarov, Y. N.; Krishnan, A. *J. Cryst. Growth* **2000**, *211*, 343.
(4) Sheldon, B. W.; Besmann, T. M.; More, K. L.; Moss, T. S. *J. Mater. Res.* **1993**, *8*, 2416.
(5) Sheldon, B. W.; Besmann, T. M.; More, K. L.; Moss, T. S. *J. Mater. Res.* **1993**, *8*, 1086.
(6) Besmann, T. M.; Sheldon, B. W.; Moss, T. S.; Kaster, M. D. *J. Am. Ceram. Soc.* **1992**, *75*, 2899.
(7) Allendorf, M. D.; Hurt, R. H.; Yang, N.; Reagan, P.; Robbins, M. *J. Mater. Res.* **1993**, *8*, 1651.
(8) Mousavipour, S. H.; Saheb, V.; Ramezani, S. *J. Phys. Chem. A* **2004**, *108*, 1946.
(9) Nitodas, S. F.; Sotirchos, S. V. *Chem. Vap. Deposition* **1999**, *5*, 219.
(10) Nitodas, S. F.; Sotirchos, S. V. *J. Electrochem. Soc.* **2000**, *147*, 1050.
(11) Nitodas, S. F.; Sotirchos, S. V. *J. Electrochem. Soc.* **2002**, *149*, C555.
(12) Nitodas, S. F.; Sotirchos, S. V. *J. Electrochem. Soc.* **2002**, *149*, C112.
(13) Nitodas, S. F.; Sotirchos, S. V. *J. Electrochem. Soc.* **2002**, *149*, C120.
(14) Papasouliotis, G. D.; Sotirchos, S. V. *J. Electrochem. Soc.* **1994**, *141*, 1599.
(15) Papasouliotis, G. D.; Sotirchos, S. V. *J. Electrochem. Soc.* **1995**, *142*, 3834.
(16) Papasouliotis, G. D.; Sotirchos, S. V. *Chem. Vap. Deposition* **1998**, *4*, 235.
(17) Papasouliotis, G. D.; Sotirchos, S. V. *J. Electrochem. Soc.* **1998**, *145*, 3908.
(18) Papasouliotis, G. D.; Sotirchos, S. V. *J. Mater. Res.* **1999**, *14*, 3397.
(19) Tsai, C. Y.; Desu, S. B.; Chiu, C. C. *J. Mater. Res.* **1994**, *9*, 104.
(20) Zhang, W. G.; Huttinger, K. J. *J. Phys. IV* **2001**, *11*, 55.
(21) Zhang, W. G. G.; Huttinger, K. J. *Chem. Vap. Deposition* **2001**, *7*, 167.
(22) Zhang, W. G. G.; Huttinger, K. J. *Chem. Vap. Deposition* **2001**, *7*, 173.
(23) Osterheld, T. H.; Allendorf, M. D.; Melius, C. F. *J. Phys. Chem.* **1994**, *98*, 6995.
(24) Mlungwane, K.; Sigalas, I. J.; Herrmann, M. *Ind. Diamond Rev.* **2005**, 62.
(25) Lin, H. F.; Xie, E. Q.; Ma, Z. W.; Zhang, J.; Peng, A. H.; He, D. Y. *Acta Phys. Sinica* **2004**, *53*, 2780.
(26) Dandekar, D. P.; Reinhart, W. D.; Chhabildas, L. C. *J. Phys. IV* **2003**, *110*, 827.
(27) Qian, J.; Voronin, G.; Zerda, T. W.; He, D.; Zhao, Y. *J. Mater. Res.* **2002**, *17*, 2153.
(28) Zhou, H.; Singh, R. N. *J. Am. Ceram. Soc.* **1995**, *78*, 2456.
(29) Josiek, A.; Langlais, F. *J. Cryst. Growth* **1996**, *160*, 253.
(30) Josiek, A.; Langlais, F.; Bourrat, X. *Chem. Vap. Deposition* **1996**, *2*, 17.
(31) Loumagne, F.; Langlais, F.; Naslain, R. *J. Cryst. Growth* **1995**, *155*, 198.
(32) Loumagne, F.; Langlais, F.; Naslain, R. *J. Cryst. Growth* **1995**, *155*, 205.
(33) Lespiaux, D.; Langlais, F. *Thin Solid Films* **1995**, *265*, 40.
(34) Langlais, F.; Loumagne, F.; Lespiaux, D.; Schamm, S.; Naslain, R. *J. Phys. IV* **1995**, *5*, 105.
(35) Loumagne, F.; Langlais, F.; Naslain, R.; Schamm, S.; Dorignac, D.; Sevely, J. *Thin Solid Films* **1995**, *254*, 75.
(36) Loumagne, F.; Langlais, F.; Naslain, R. *J. Phys. IV* **1993**, *3*, 527.
(37) Bouillon, E.; Langlais, F.; Pailler, R.; Naslain, R.; Cruege, F.; Huong, P. V.; Sarthou, J. C.; Delpuech, A.; Laffon, C.; Lagarde, P.; Monthioux, M.; Oberlin, A. *J. Mater. Sci.* **1991**, *26*, 1333.
(38) Langlais, F.; Prebende, C.; Tarride, B.; Naslain, R. *J. Phys.* **1989**, *50*, 93.
(39) From http://www.camd.lsu.edu/msds/s/silicon_carbide.htm on 2/28/2006.
(40) Lide, D. R. *CRC Handbook of Chemistry and Physics*, 86th ed.; CRC Press: Boca Raton, FL, 2005−2006.
(41) Aikens, C. M.; Webb, S. P.; Bell, R. L.; Fletcher, G. D.; Schmidt, M. W.; Gordon, M. S. *Theor. Chem. Acc.* **2003**, *110*, 233.
(42) Dunning, T. H. *J. Chem. Phys.* **1989**, *90*, 1007.
(43) Woon, D. E.; Dunning, T. H. *J. Chem. Phys.* **1993**, *98*, 1358.
(44) Schmidt, M. W.; Baldridge, K. K.; Boatz, J. A.; Elbert, S. T.; Gordon, M. S.; Jensen, J. H.; Koseki, S.; Matsunaga, N.; Nguyen, K. A.; Su, S. J.; Windus, T. L.; Dupuis, M.; Montgomery, J. A. *J. Comput. Chem.* **1993**, *14*, 1347.
(45) ACES II is a program product of the Quantum Theory Project, University of Florida. Authors: J. F. Stanton, J. Gauss, J. D. Watts, M. Nooijen, N. Oliphant, S. A. Perera, P. G. Szalay, W. J. Lauderdale, S. A. Kucharski, S. R. Gwaltney, S. Beck, A. Balková D. E. Bernholdt, K. K. Baeck, P. Rozyczko, H. Sekino, C. Hober, and R. J. Bartlett. Integral packages included are VMOL (J. Almlöf and P. R. Taylor); VPROPS (P. Taylor) ABACUS; (T. Helgaker, H. J. Aa. Jensen, P. Jørgensen, J. Olsen, and P. R. Taylor).
(46) Bode, B. M.; Gordon, M. S. *J. Mol. Graphics Modell.* **1998**, *16*, 133.
(47) Experimental values are at 298.15, 300, 400, ..., 1500 K. Thermodynamic properties were calculated at 298.15, 400, 600, ..., 2000 K. Direction experimental and theoretical comparison can be made at 298.15, 400, 600, 800, 1000, 1200, and 1400 K.
(48) From http://kinetics.nist.gov/ on 2/28/2006.
(49) Martin, J. M. L. *Chem. Phys. Lett.* **1996**, *259*, 669.
(50) Blanksby, S. J.; Ellison, G. B. *Acc. Chem. Res.* **2003**, *36*, 255.